

AN ABSTRACT OF THE THESIS OF

Stephen Robert Ely for the degree of Doctor of Philosophy
in Chemistry presented on October 15, 1975

Title: NOVEL LANTHANIDE COMPOUNDS WITH π -LIGANDS.

I. THE REACTIONS OF LANTHANUM, NEODYMIUM AND
ERBIUM ATOMS WITH CYCLOOCTATETRAENE. II. THE
REACTIONS OF NEODYMIUM AND ERBIUM CHLORIDES
WITH THE DICARBOLLIDE ION.

Abstract approved: *Redacted for Privacy*
Dr. Carroll W. DeKock

Lanthanum, neodymium and erbium atoms react with cyclooctatetraene, COT, at -196°C to form a new class of lanthanide COT compounds, $\text{Ln}_2(\text{COT})_3$. These compounds are extremely air and moisture sensitive, are insoluble in nonpolar solvents, but are sparingly soluble in tetrahydrofuran, THF. The lanthanum and neodymium members of the series crystallize from THF with two solvent molecules. Physical and chemical evidence are consistent with ionic bonding. A single crystal X-ray determination of the neodymium compound was done. It revealed that the molecules exist as anion-cation pairs, $[\text{Nd}(\text{COT})_2]^-$ and $[\text{Nd}(\text{COT})(\text{THF})_2]^+$. All COT rings are present as the ten π -electron aromatic dianion. The present structure exhibits two distinct differences from those of

other lanthanide and actinide COT compounds. First, the COT²⁻ rings in the anion are neither equidistant from the anion Nd nor parallel. The average Nd1-C distances are 2.66 (2) Å and 2.79 Å for rings 1 and 2. The ring planes intersect at an angle of 8.25°. Second, the cation is asymmetrically located with respect to ring 2. Nd2-ring 2 distances range from 2.70 (2) Å to 4.67 Å. These differences are explained by electrostatic and steric considerations. The crystals have the following data: monoclinic space group P2₁/c, cell constants a = 16.664 (3), b = 12.778 (3), c = 14.370 (4) Å, β = 108.90 (2)°, z = 4, ρ_{obsd} = 1.75, ρ_{calc} = 1.71 g/cm³. The structure has been refined with full-matrix least-squares methods using 3351 independent and non-zero reflections. For the 1371 reflections whose F² > 3σ(F²), the standard unweighted R factor is 3.30%.

The products of the reactions of NdCl₃ and ErCl₃ with the dicarbollide ion, B₉C₂H₁₁²⁻, are dependent on the mole ratio of the reactants. When the mole ratio of NdCl₃ and ErCl₃ to B₉C₂H₁₁²⁻ is 2:1, the products are [NaN₂Cl₂(B₉C₂H₁₁)·THF]₂·NdCl₃ and NaErCl₂(B₉C₂H₁₁)·THF. These two compounds represent the first lanthanide carboranes and the first chloro-metallo-dicarbollides. With the mole ratio of 1:3 the products are Na₃Nd(B₉C₂H₁₁)₃·2THF and Na₃Er(B₉C₂H₁₁)₃·THF. The displacement of chloride from NdCl₃ and ErCl₃ by dicarbollide has been shown to be an irreversible stepwise process. The difference in product formation between

NdCl_3 and ErCl_3 under similar reaction conditions is attributed to the differences in ionic size between Nd^{3+} and Er^{3+} caused by the lanthanide contraction.

Novel Lanthanide Compounds with π -Ligands. I. The Reactions
of Lanthanum, Neodymium and Erbium Atoms with
Cyclooctatetraene. II. The Reactions of
Neodymium and Erbium Chlorides with
the Dicarbolide Ion

by

Stephen Robert Ely

A THESIS

submitted to

Oregon State University

in partial fulfillment of
the requirements for the
degree of

Doctor of Philosophy

June 1976

APPROVED:

Redacted for Privacy

Associate Professor of Chemistry

in charge of major

Redacted for Privacy

Chairman of Department of Chemistry

Redacted for Privacy

Dean of Graduate School

Date thesis is presented October 15, 1975

Typed by Clover Redfern for Stephen Robert Ely

ACKNOWLEDGMENTS

I am very pleased to share the credit for this thesis with Carroll DeKock. His guidance and assistance throughout the course of the experimental work and preparation of this manuscript have helped make it possible. I also thank him for his interest in and concern for me and my family.

I cherish the patience, understanding and affection my wife, Pat, has shown these past four years.

I owe special thanks to Ted Hopkins for all his help with the crystal structure determination and to John Yoke for being my "foster father" for a year.

I would also like to thank Clara and David Shoemaker, Ingo Joedicke, Mike Lesiecki, Lou Allamandola, Susan Randall and Susan Critchlow for the help each has given.

I am grateful for the financial support of the Petroleum Research Foundation, the Energy Research and Development Administration and last, but by no means least, the people of the state of Oregon, whose tax dollars help support this institution.

To Pat and Meredith

TABLE OF CONTENTS

	<u>Page</u>
PART I: THE REACTIONS OF LANTHANUM, NEODYMIUM AND ERBIUM ATOMS WITH CYCLOOCTATETRAENE	1
INTRODUCTION	2
EXPERIMENTAL	7
Materials	7
Reactions	8
Preparation of LnCp_3	10
Preparation of $[\text{Ln}(\text{COT})(\text{THF})_2][\text{Ln}(\text{COT})_2]$	11
Reaction of Er with COT	14
Attempted Preparation of $\text{NdCp}(\text{COT})$	14
Analyses	15
Physical Measurements	16
Structure of $[\text{Nd}(\text{COT})(\text{THF})_2][\text{Nd}(\text{COT})_2]$	17
X-ray Data Collection and Reduction	17
Solution and Refinement of the Structure	20
RESULTS AND DISCUSSION	24
Physical Properties of $[\text{Ln}(\text{COT})(\text{THF})_2][\text{Ln}(\text{COT})_2]$	
Compounds	24
Analytical Results	24
Structure of $[\text{Nd}(\text{COT})(\text{THF})_2][\text{Nd}(\text{COT})_2]$	25
Structure of $[\text{La}(\text{COT})(\text{THF})_2][\text{La}(\text{COT})_2]$	34
Infrared Spectra	36
Raman Spectra	36
Nuclear Magnetic Resonance	39
Magnetic Susceptibility	40
Chemical Properties and Reactions	40
Thermal Decomposition	40
Hydrolysis	41
Oxidation	41
Reaction with UCl_4	42
CONCLUSIONS	43

PART II: THE REACTIONS OF NEODYMIUM AND ERBRIUM CHLORIDES WITH THE DICARBOLLIDE ION

INTRODUCTION	45
THE NdCl_3 -DICARBOLLIDE ION SYSTEM	50
Experimental	50
Materials	50
Preparation of $[\text{NaNdCl}_2(\text{B}_9\text{C}_2\text{H}_{11}) \cdot \text{THF}]_2 \cdot \text{NdCl}_3$, (I)	51
Preparation of $\text{Na}_3\text{Nd}(\text{B}_9\text{C}_2\text{H}_{11})_3 \cdot 2\text{THF}$, (II)	51
Reaction of $[\text{NaNdCl}_2(\text{B}_9\text{C}_2\text{H}_{11}) \cdot \text{THF}]_2 \cdot \text{NdCl}_3$, (I), with $\text{Na}_2\text{B}_9\text{C}_2\text{H}_{11}$	52
Attempted Reaction of $\text{Na}_3\text{Nd}(\text{B}_9\text{C}_2\text{H}_{11})_3 \cdot \text{THF}$, (III), with NdCl_3	52
Reaction of $[\text{NaNdCl}_2(\text{B}_9\text{C}_2\text{H}_{11}) \cdot \text{THF}]_2 \cdot \text{NdCl}_3$, (I), with NaCp	53
Analyses	53
Physical Measurements	54
Summary	54
THE ErCl_3 -DICARBOLLIDE ION SYSTEM	60
Experimental	60
Materials	60
Preparation of $\text{NaErCl}_2(\text{B}_9\text{C}_2\text{H}_{11}) \cdot \text{THF}$, (III)	60
Preparation of $\text{Na}_3\text{Er}(\text{B}_9\text{C}_2\text{H}_{11})_3 \cdot \text{THF}$, (IV)	61
Attempted Reaction of $\text{Na}_3\text{Er}(\text{B}_9\text{C}_2\text{H}_{11})_3 \cdot \text{THF}$, (IV), with ErCl_3	62
Reaction of $\text{NaErCl}_2(\text{B}_9\text{C}_2\text{H}_{11}) \cdot \text{THF}$, (II), with NaCp	62
Thermal Decomposition of $\text{NaErCl}_2(\text{B}_9\text{C}_2\text{H}_{11}) \cdot \text{THF}$, (II)	62
Analyses	62
Physical Measurements	63
Summary	63
DISCUSSION AND CONCLUSIONS	66
BIBLIOGRAPHY	70
APPENDIX	75

LIST OF FIGURES

<u>Figure</u>	<u>Page</u>
1. A schematic drawing of the metal atom reaction vessel.	9
2. A schematic drawing of the Soxhlet extractor used for the purification and crystallization of $[\text{Ln}(\text{COT})(\text{THF})_2][\text{Ln}(\text{COT})_2]$ compounds.	12
3. A perspective view of $[\text{Nd}(\text{COT})(\text{THF})_2][\text{Nd}(\text{COT})_2]$.	26
4. A perspective view of the packing of $[\text{Nd}(\text{COT})(\text{THF})_2][\text{Nd}(\text{COT})_2]$ as viewed down the b-axis.	35
5. Raman spectrum of $[\text{Nd}(\text{COT})(\text{THF})_2][\text{Nd}(\text{COT})_2]$.	38
6. A schematic drawing of $(3)\text{-}1,2\text{-B}_9\text{C}_2\text{H}_{11}^{2-}$, the dicarbollide ion, showing approximately sp^3 hybrid orbitals directed at the vacant (3)-vertex.	47

LIST OF TABLES

<u>Table</u>	<u>Page</u>
1. Analytical results on COT compounds.	16
2. Summary of crystal data.	19
3. Positional and thermal parameters.	22
4. Root-mean-square amplitudes of vibration along the principal axes in units of Angstroms	23
5. Bond lengths and angles in cyclooctatetraene rings.	27
6. Least-squares planes of cyclooctatetraene rings.	28
7. Neodymium-carbon distances.	29
8. Bond lengths and angles for tetrahydrofuran rings.	33
9. Infrared spectra of COT compounds.	37
10. Powder pattern data for dicarbollide compounds.	56
11. Visible spectra of dicarbollide compounds.	58
12 ^{11}B nmr data.	59

PART I

THE REACTIONS OF LANTHANUM, NEODYMIUM
AND ERBIUM ATOMS WITH
CYCLOOCTATETRAENE

NOVEL LANTHANIDE COMPOUNDS WITH π -LIGANDS

INTRODUCTION

In 1963 Skell and Wescott [1] first reported that carbon vapor, formed from a carbon arc under high vacuum, reacted with organic compounds at -196°C to give new compounds incorporating the vapor species. The carbon was vaporized under high vacuum so that the vapor species could move away from the arc without intermolecular collisions which would have caused aggregation. The walls of the surrounding vessel were maintained at -196°C . Reactant vapors were passed into the vessel while the carbon was vaporizing and were condensed sufficiently rapidly that the high vacuum was maintained. A combination of high pumping speed and the -196°C walls allowed substantial rates of addition of the reactants with very few gas phase collisions. Reaction occurred on the vessel walls provided thermodynamic and kinetic factors were favorable.

This work marked the beginning of what has proved to be a fruitful area of research [2, 3, 4]. Using conditions similar to those of Skell and Wescott over 25 high temperature species have been used as synthetic reagents for the preparation of many known and new compounds.

For the last six or seven years, metal atoms have received the most attention as the high temperature species of interest. Some results of this rapidly growing field were featured in the symposium "Metal Atoms in Chemical Synthesis" held under the auspices of the Merck'sche Gesellschaft für Kunst and Wissenschaft e.V. at Darmstadt, May 12-15, 1974 [5].

Metal atoms can be expected to be more reactive than the bulk metal for two reasons. First, the atom is less sterically hindered and generally has readily available electrons. Second, the atom is a higher energy species. This energy is expected to be approximately the heat of formation of the gaseous atom, as condensation of the atoms in an inert atmosphere at -196°C will not greatly affect their energy. For the metals used in this study, the heats of vaporization in kcal/mole are 104, 77 and 75 for La, Nd and Er, respectively [6]. This energy supplied the atoms is great enough to allow the formation of products that can not be formed from the reaction of the bulk metal with the organic substrate under normal conditions.

A few examples include such well known compounds as ferrocene [7] and bis(benzene)chromium [8] and such new and exciting compounds as bis(arene)titanium [9], which has been shown to catalyze the oligerimization of butadiene, and tris(butadiene)tungsten and molybdenum [10].

Since the reported preparation of di- π -cyclooctatetraeneuranium (IV), uranocene [11], in 1968, there has been a renaissance of interest in organolanthanide and actinide chemistry [12].

The preparations of π -carbocyclic compounds and the preparations of σ -bonded alkyl compounds have received the most attention. Streitwieser and coworkers have been interested in the possibility of f-orbital bonding and have made comparisons of lanthanide and actinide π -cyclooctatetraene compounds, $\text{KLn}(\text{COT})_2$ [13] and $\text{U}(\text{COT})_2$ [14]. Tsutsui [15, 16, 17], Marks [18] and coworkers have recently prepared a number of σ -bonded alkyl compounds of the type LnCp_2R and UCp_3R , where Cp^- is the cyclopentadienide ion, C_5H_5^- .

The purpose of this work was to couple these active areas of research and to synthesize organolanthanide compounds using the metal atoms as one of the reagents. Since this work was begun, there have been what the author believes to be the first reports of work with lanthanide atoms. The atoms have been codeposited with CO in an argon matrix [19, 20] and with benzene [21]. The systems chosen for study were the reactions of La, Nd and Er atoms with cyclopentadiene and cyclooctatetraene.

Nd and Er, ionic radii equal 0.995 \AA and 0.881 \AA , respectively, were chosen so as to observe possible differences in reactivity or product formation between light and heavy lanthanides due to the

lanthanide contraction. Lanthanide contraction consists of a significant and steady decrease in the size of the atoms and ions with increasing atomic number caused by the imperfect shielding of 4f electrons by one another. Differences in certain chemical properties of lanthanide compounds have been attributed to this contraction. For example, the reactions of NaCp with LnCl_3 gives only LnCp_3 for the light lanthanides but give LnCp_3 , LnCp_2Cl and LnCpCl_2 for the heavier lanthanides [22, 23]. La, ionic radius equals 1.061 Å, was later used in hopes of preparing diamagnetic species so as to observe the proton magnetic resonances and to gain structural information.

To serve as a useful check on our technique, LaCp_3 , NdCp_3 and ErCp_3 were prepared by cocondensing the metal atoms with cyclopentadiene.

Cyclooctatetraene, COT, was chosen for two reasons. First, three types of lanthanide COT compounds were known, $\text{Ln}(\text{COT})$ ($\text{Ln}=\text{Eu}, \text{Yb}$) [24], $\text{KLn}(\text{COT})_2$ ($\text{Ln}=\text{Y}, \text{La}, \text{Ce}, \text{Pr}, \text{Nd}, \text{Sm}, \text{Gd}, \text{Tb}$) [13] and $[\text{Ln}(\text{COT})\text{Cl} \cdot 2\text{THF}]_2$ ($\text{Ln}=\text{Ce}, \text{Pr}, \text{Nd}, \text{Sm}$) [13]. Crystal structures of $[\text{K}(\text{diglyme})][\text{Ce}(\text{COT})_2]$ [25] and $[\text{Ce}(\text{COT})\text{Cl} \cdot 2\text{THF}]_2$ [26] have also been reported. Since this work was begun an additional type of compound, $\text{LnCp}(\text{COT})$, has been reported [27]. Second, it was felt that because the normal oxidation state of the lanthanides is +3 and knowing that COT can readily be reduced to a ten π -electron aromatic dianion, there would be a real

possibility of forming compounds with the empirical formula, $\text{Ln}_2(\text{COT})_3$. Furthermore it was hoped that such compounds would have triple decker sandwich structures. There has been one previous report of $\text{M}_2(\text{COT})_3$ ($\text{M}=\text{Ti}, \text{Cr}, \text{Mo}, \text{W}$) compounds [28]. In $\text{Ti}_2(\text{COT})_3$ the outer rings are planar and aromatic, but the central ring is twisted as to create a two fold axis of symmetry [29].

This investigation resulted in an alternate synthesis of La, Nd and Er cyclopentadienides and the preparation of $[\text{La}(\text{COT})(\text{THF})_2][\text{La}(\text{COT})_2]$, $[\text{Nd}(\text{COT})(\text{THF})_2][\text{Nd}(\text{COT})_2]$ and $\text{Nd}_2(\text{COT})_3$, members of a new class of π -carbocyclic lanthanides.

The crystal and molecular structure of $[\text{Nd}(\text{COT})(\text{THF})_2][\text{Nd}(\text{COT})_2]$ has been determined from three-dimensional X-ray data collected by counter methods. The crystals belong to the monoclinic space group $\text{P}2_1/\text{c}$, with cell constants $a = 16.664(3)$, $b = 12.778(3)$, $c = 14.370(4)$, $\beta = 108.90(2)$. For four formula units per unit cell, the calculated density is 1.71 g/cm^3 . The observed density is 1.75 g/cm^3 . The structure has been refined with full-matrix least-squares methods using 3351 independent and non-zero reflections. For the 1371 reflections whose $F^2 > 3\sigma(F^2)$, the standard unweighted R factor is 3.30%.

The structure is different from either the hoped for triple decker or that of the $\text{Ti}_2(\text{COT})_3$ [29]. Rather the molecule consists of an anion-cation pair. The anion is $[\text{Nd}(\text{COT})_2]^-$ and the cation is $[\text{Nd}(\text{COT})(\text{THF})_2]^+$.

EXPERIMENTAL

Materials

La, Nd and Er, 99.9%, were obtained from Michigan Chemical Corporation, St. Louis, Michigan, and Research Chemicals, Phoenix, Arizona.

CpH was obtained by distillation of dicyclopentadiene (Eastman Organic Chemicals) immediately before use.

COT, generously donated by Dr. E.N. Marvell of this department, was dried over molecular sieve and used without further purification.

THF (Mallinkroft Analytical Reagent Grade) was refluxed over LiAlH_4 and stored under vacuum over LiAlH_4 for at least two days before it was used.

KBr (Harshaw, Infrared Quality) was dried at 150°C at 10^{-4} mm Hg for several days and stored in the inert atmosphere box until used.

UCl_4 was purchased from Research Organic Inorganic Chemicals, Sun Valley, California, and used without further purification.

Prepurified Grade nitrogen (Air Reduction Company) was used as received. The maximum oxygen content is guaranteed by the supplier to be less than 8 ppm.

Reactions

All metal atom reactions were carried out in the reaction vessel shown in Figure 1. The vessel was constructed using a Pyrex two liter round bottom flask and a three-inch glass pipe flange. The vessel is equipped with three ports and a removable back plate. The one inch port is used for constant pumping on the system during the deposit. One 3/8-inch port is used for volatile product pump out and the second 3/8-inch port, not shown in the drawing, is fitted with a H.S. Martin and Son Model #M-40312 cold cathode gauge and a dry nitrogen inlet. Port connections are made using Cajon ultra-torr fittings. The back plate is vacuum fitted to the flange using an aluminum collar and O-rings. A 1/8-inch copper tube, through which the organic substrate is introduced, and two water cooled copper electrodes are in the back plate. Adequate dispersion of the organic substrate is obtained by placing a tee and numerous holes in the 1/8-inch line. The metal atoms are generated by resistively heating a Sylvania Type BC 10064X30 tungsten basket which is attached to the electrodes with stainless steel screws and washers. The power source is a transformer which steps down the line voltage to 10 volts and is further controlled by means of a variac.

Because of the geometry of the assembly, no more than 75% of the metal atoms reach the flask walls for reaction. The atoms not

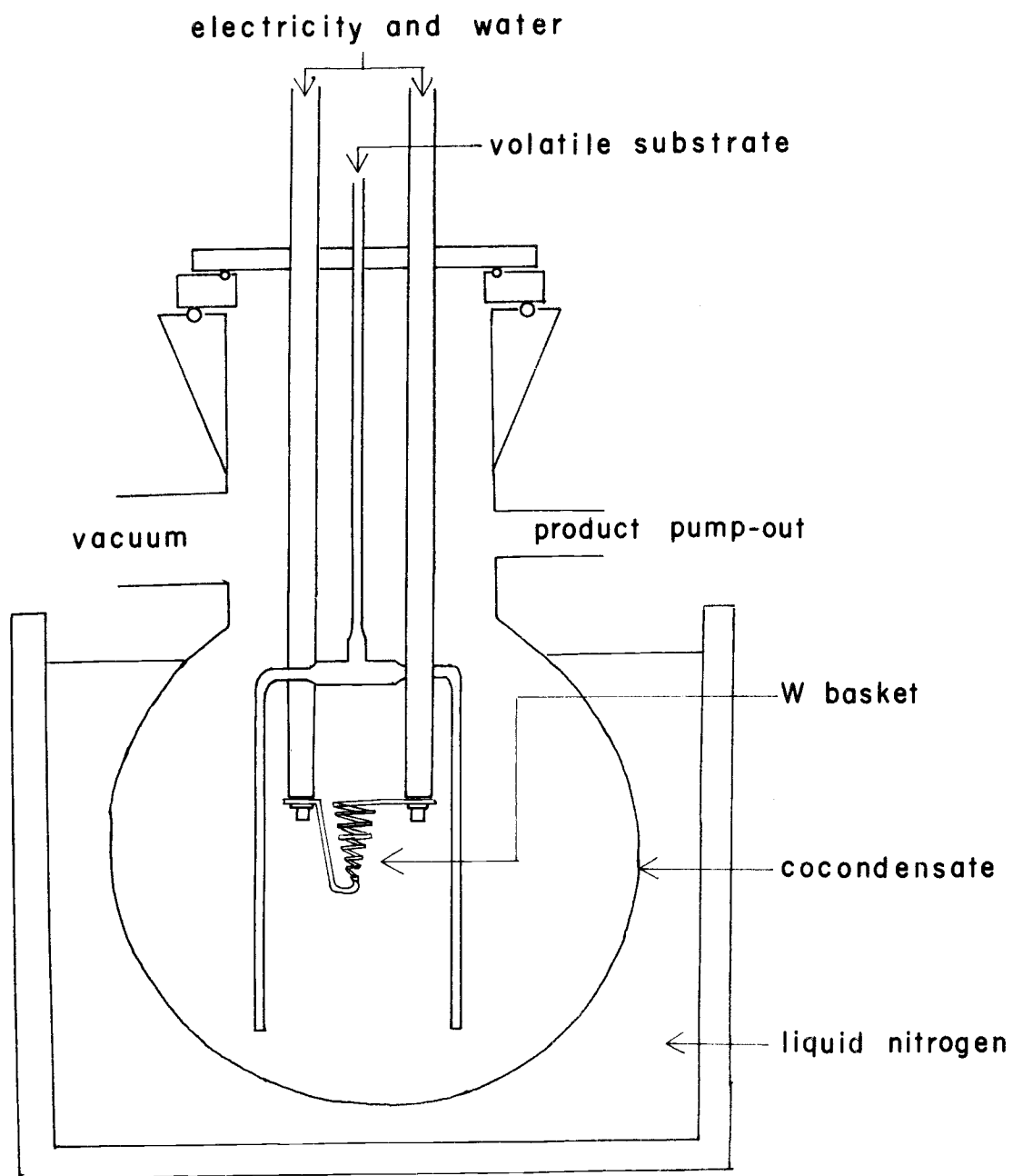


Figure 1. A schematic drawing of the metal atom reaction vessel.

reaching the flask walls condense on the inlet tube, the electrodes and the back plate.

Following cocondensation of the reactants, the flask was allowed to warm to room temperature and the volatile materials pumped out under vacuum. The vessel was filled with nitrogen and, taking extreme precautions to exclude air by carefully capping all ports, was transferred to a Forma Scientific Model #3818 stainless steel inert atmosphere box fitted with a #3851 evacuable interchange assembly and an oxygen and moisture free recirculating nitrogen atmosphere

The distinct advantage of this vessel is its size. It is large enough so that millimole quantities of product can be made, yet small enough to be easily moved into the inert atmosphere box. This allows the isolation and study of nonvolatile, air-sensitive, reaction products. The author knows of no other investigators in the area of metal atom chemistry with this capability.

Preparation of LnCp_3

The procedure was identical for the three metals studied. Fifteen ml (200 mmoles) of freshly distilled CpH and 0.5-0.7 g (3-5 mmoles) La, Nd or Er were cocondensed at -196°C for approximately 1 hour. No H_2 was evolved during this period. When the contents of the flask were allowed to warm, reaction was initiated. H_2 was

evolved and the black matrix turned white, blue or pink for La, Nd or Er, respectively. Following removal of the excess CpH, the vessel was transferred to the inert atmosphere box and the solid product was placed in a sublimator. The sublimed products were characterized by their infrared and visible spectra as LaCp_3 , NdCp_3 and ErCp_3 , respectively [31,32]. Because the LnCp_3 compounds are well known, no further discussion of their properties will be given.

Preparation of $[\text{Ln}(\text{COT})(\text{THF})_2][\text{Ln}(\text{COT})_2]$

Fifteen ml (130 mmoles) COT and 1.0-2.0 g (7-14 mmoles) La or Nd were cocondensed at -196°C for 30-60 minutes. The pressure inside the reaction vessel was kept below 4×10^{-4} mm Hg. Higher pressures led to the polymerization of COT as the predominant reaction. Reaction apparently takes place on the vessel walls at -196°C as evidenced by the immediate formation of a gold colored substance with La and a bright green colored substance with Nd. The vessel was warmed to room temperature and the excess COT removed leaving nonvolatile, extremely air and moisture sensitive, gold solids.

The vessel was transferred to the inert atmosphere box and the solid was placed in a Soxhlet extractor designed for continuous extraction through a sinter-glass filter.

The extractor is shown in Figure 2. The basic design of the extractor is the same as that of the extractor used by Streitwieser and

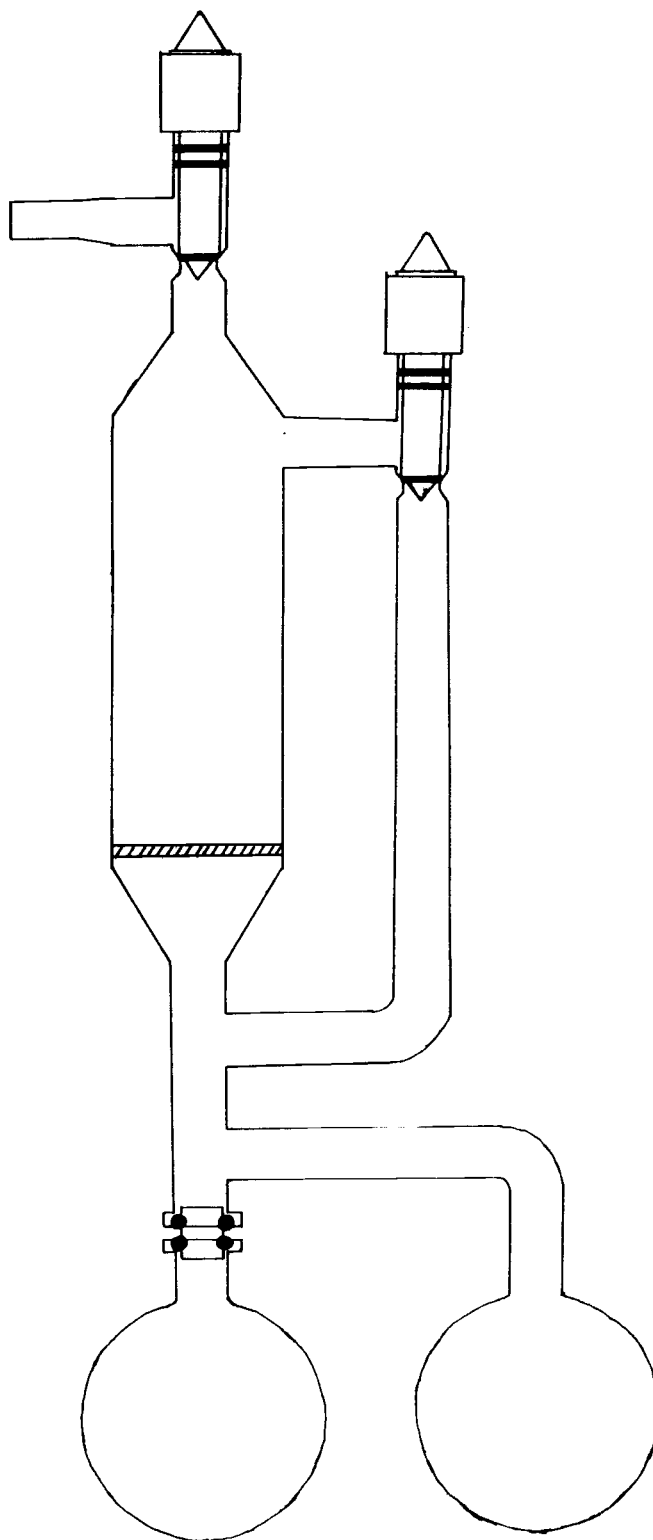


Figure 2. A schematic drawing of the Soxhlet extractor used for the purification and crystallization of $[\text{Ln}(\text{COT})(\text{THF})_2][\text{Ln}(\text{COT})_2]$ compounds.

coworkers for the purification of $\text{U}(\text{COT})_2$ [14]. Two major improvements have been made. First, the pure product is contained in a flask which is connected to the body of the extractor via a Fischer-Porter Solv-seal teflon joint. This joint allows easy removal of the flask without having to break the extractor. Second, the extractor has two J. Young Action Type POR/10mm/RA valves purchased from Chemvac Associates, Columbus, S.C. These valves have teflon O-ring seals and seats which allow a grease free system.

After transfer of the solid, the extractor was removed from the box and was evacuated. Seventy-five ml of THF was vacuum transferred into the extractor and the extractor was sealed. The atmosphere within the extractor consisted of only solvent vapor. This allowed operating temperatures below the normal boiling point of the solvent, an important feature as thermal stability of the product was a problem. This also eliminated problems caused by maintaining a positive pressure on the system.

The first two or three extractions, containing dark yellow impurities, were poured into the side arm. These impurities were assumed to be polymeric material. Following these extractions, the solution passing the filter was nearly colorless. Gold crystals of $[\text{La}(\text{COT})(\text{THF})_2][\text{La}(\text{COT})_2]$ or green crystals of $[\text{Nd}(\text{COT})(\text{THF})_2][\text{Nd}(\text{COT})_2]$ grew during the 7-10 day extraction.

After extraction, the THF was poured into the side arm. Small amounts of THF were distilled back from the side arm and the crystals washed. The washings were again poured into the side arm. The crystals were washed at least twice in this manner. The combined solutions in the side arm were reduced to near dryness under vacuum. Finally, the extractor was taken to the inert atmosphere box and the crystals were removed.

Reaction of Er with COT

The reaction was done in the same manner as the La and Nd reactions. The infrared spectrum and the chemical properties of the crude product indicated the presence of COT^{2-} (vide infra). No attempt to grow crystals was made.

Attempted Preparation of $\text{NdCp}(\text{COT})$

Several attempts were made to prepare the mixed sandwich compound, $\text{NdCp}(\text{COT})$, by cocondensing Nd, CpH and COT. Infrared spectra of the products indicated the presence of Cp^- and COT^{2-} . However no evidence was found to rule out the possibility that the observed spectrum was not due entirely to a mixture of NdCp_3 and $\text{Nd}_2(\text{COT})_3$. At the time this work was done, Takats and coworkers [27] reported the preparation of several $\text{LnCp}(\text{COT})$ compounds. Therefore no further work on this system was done.

Analyses

Because the COT compounds are extremely air and moisture sensitive, commercial analyses were unsatisfactory. Streitwieser has observed the same difficulty with his COT compounds [13, 14]. The methods listed below gave satisfactory results.

Metal analyses were accomplished using back complexometric titration procedures with disodium EDTA [33]. Approximately 100 mg of sample was weighed on a Mettler Type H16 balance. Two ml of distilled water was vacuum transferred onto the weighted sample. The hydrolysis products were dissolved in dilute HNO_3 and diluted to 100 ml. Twenty ml aliquots were treated with excess 0.01M Na_2EDTA , 10 ml, and buffered to pH = 8.4-8.7 with $\text{NH}_4\text{Cl}-\text{NH}_4\text{OH}$. Two drops of 1% Eriochrome black-T in 2,2',2''-nitrilotriethanol was added as the indicator. The solution was titrated with 0.01M ZnCl_2 until the blue color had completely changed to pink, 5 ml. End points were found to be sharper if nitrogen was slowly bubbled through the solution. Results are presented in Table 1.

COT^{2-} analyses were accomplished by the careful hydrolysis of weighed samples. The yellow organic layer was extracted into CCl_4 , to which a weighed amount of benzene had been added. Assuming quantitative conversion of COT^{2-} to cyclooctatrienes, the results presented in Table 1 were obtained by comparison of the pmr peak

intensities of the benzene and the cyclooctatrienes.

Table 1. Analytical results on COT compounds.

Compound		% Ln	% COT	% THF
[La(COT)(THF) ₂][La(COT) ₂]	calc.	37.83	42.54	19.63
	found	39.24	34.3 ^a	21.7
[Nd(COT)(THF) ₂][Nd(COT) ₂]	calc.	38.72	41.93	19.35
	found	39.33	40.7	20.4
Nd ₂ (COT) ₃	calc.	48.01		
	found	46.94		

^aIncomplete hydrolysis. See Results and Discussion section.

THF analyses were accomplished by treating weighed samples with a weighed solution of benzene in acetone-d₆. After reaction had ceased the volatile materials were vacuum transferred to an nmr tube. The peak intensities of benzene and the α-protons of the THF were compared. Results are presented in Table 1.

Physical Measurements

Infrared spectra were recorded as KBr pellets on a Perkin Elmer 621 grating spectrophotometer and calibrated versus polystyrene. Maxima are believed to be accurate to $\pm 2 \text{ cm}^{-1}$.

Visible spectra of NdCp₃ and ErCp₃ were recorded as THF solutions at room temperature on a Cary 15 spectrophotometer using 1-cm silica cells.

The Raman spectrum of $[\text{Nd}(\text{COT})(\text{THF})_2][\text{Nd}(\text{COT})_2]$ was recorded on a sample sealed in a glass tube with a Cary 82 spectrophotometer using the 6471 \AA exciting line of a Spectra Physics Model 164 Krypton ion laser operating at 100 mW. No Raman spectrum of $[\text{La}(\text{COT})(\text{THF})_2][\text{La}(\text{COT})_2]$ could be obtained because of fluorescence.

NMR spectra were recorded either on a Varian HA-100 or EM 360 spectrometer.

The magnetic susceptibility of $[\text{Nd}(\text{COT})(\text{THF})_2][\text{Nd}(\text{COT})_2]$ was measured at 16°C on a sample sealed in a glass tube using a Faraday susceptibility apparatus by Dr. John Gardner of the Physics Department of this University.

X-ray power diffraction patterns were obtained using a General Electric Diffraction Unit. Sealed capillaries were used in a 114.6 mm diameter powder camera with nickel filtered Cu K_α radiation. Values of d-spacings were calculated from the Bragg equation.

Structure of $[\text{Nd}(\text{COT})(\text{THF})_2][\text{Nd}(\text{COT})_2]$

X-ray Data Collection and Reduction

Several crystals were sealed in 0.3 mm glass capillaries under a nitrogen atmosphere. In order to hold the crystals in place, the inside walls had been coated with a thin layer of Dow Corning Silicone

High Vacuum Lubricant. The capillaries were outgassed at 80-100°C at 10^{-4} mm Hg overnight before they were taken to the inert atmosphere box.

The crystal chosen for study was mounted on a Syntex $\overline{\text{P1}}$ computer-controlled four circle diffractometer [34]. A three hour exposure orientation photograph was taken using graphite-monochromatized Mo K_α radiation. The unit cell parameters were initially determined using the reflections from the photograph. A preliminary set of reflections were measured to determine the space group. These reflections showed monoclinic symmetry with the following systematic absences: $h0l$, $l \neq 2n$; $0k0$, $k \neq 2n$. Space group $\text{P2}_1/\text{c}$, number 14, is the only choice which is consistent with these conditions. This was subsequently verified by the complete crystal structure determination.

The final unit cell constants and orientation matrix were determined by a least-squares refinement of 15 reflections whose 2θ angles ranged from 12-22°. The resulting cell parameters and other pertinent data are presented in Table 2.

Intensity data were collected using a θ - 2θ scan mode with a scintillation counter. The 2θ scans for each reflection were from 1° below the $\text{K}_{\alpha 1}$ peak to 1° above the $\text{K}_{\alpha 2}$ peak with a scan rate of 1°/minute. The background counting time was equal to the scan time for each reflection. All independent reflections in the sphere

$0^\circ \leq 2\theta \leq 42.5^\circ$ and about 150 reflections in the sphere $42.5 \leq 2\theta \leq 45^\circ$ were collected. During the experiment, the intensities of the 012, $\bar{1}02$ and $7\bar{1}4$ reflections were measured every 50 reflections as a check on the stability of the crystal and the instrument. Of the 4203 total reflections collected, 3541 were independent and 3351 were both independent and non-zero.

Table 2. Summary of crystal data.

Molecular formula:	$[\text{Nd}(\text{COT})(\text{THF})_2][\text{Nd}(\text{COT})_2]$
Molecular weight:	745.13
Linear absorption coefficient, μ :	33.18 cm^{-1}
Observed density: ^a	1.75 g/cm^3
Calculated density:	1.71 g/cm^3
Crystal dimensions:	$0.3 \times 0.08 \times 0.08 \text{ mm}$
Space group:	$P2_1/c$, monoclinic
Molecules/unit cell:	4
Cell constants: ^b	$a = 16.664 (3), b = 12.778 (3), c = 14.3470 (4) \text{ \AA};$ $\beta = 108.90 (2)^\circ; \cos \beta = 0.32393$
Cell volume:	2894.74 \AA^3

^a Experimental density measurements were obtained by floatation measurements in $\text{CCl}_4\text{-CBr}_4$.

^b Mo $K_{\alpha 1}$ radiation, $\lambda = 0.70926 \text{ \AA}$. Ambient temperature of 21°C .

STUDIT, a program which averages intensities with identical and point-group-equivalent indices, and INCOR, a program which applies the Lorentz and polarization factors were used in the data reduction. Coefficients for a sharpened Patterson function and E

coefficients were calculated using PASHCO. The above calculations were done locally on a CDC 3300 computer.

Solution and Refinement of the Structure

The solution and refinement calculations were done on a CDC 7600 computer at the University of California, Berkeley. The programs used are part of the X-ray crystallographic library maintained by Dr. Allan Zalkin. Connection with the 7600 was made using the facilities of the Environmental Protection Agency, Corvallis, Oregon. I would like to thank the people at Berkeley and the EPA for the use of their facilities.

The positions of the Nd atoms were determined directly from an E map using the phases calculated by MULTAN for the 300 largest E coefficients from PASHCO. These positions were checked against a three-dimensional Patterson map and were consistent with the major peaks. Anisotropic least-squares refinement on these two atoms using LSLONG, followed by difference Fourier synthesis on F using FORDAP, located the two THF oxygen atoms and 22 COT carbon atoms. Three additional least-squares cycles with the neodymiums anisotropic and other atoms isotropic and another difference Fourier located the remaining carbon atoms. No attempt was made to locate the H atoms.

Full-matrix least-squares refinements of F were used in which the function minimized was $\sum w(|F_o| - |F_c|)^2$, where F_o and F_c are the observed and calculated structure factors. The weighting factor, w , is $1/\sigma^2(F_o)^2$. The scattering factors for Nd^{3+} and neutral O and C were taken from the values tabulated by Cromer and Mann [35]. Anomalous dispersion corrections, $\Delta f'$ and $\Delta f''$ were taken from the values tabulated in the International Tables [36]. The final agreement factors $R_1 = \sum ||F_o| - |F_c|| / \sum |F_o|$ and R_2 (weighed R factor) = $[\sum w(|F_o| - |F_c|)^2 / \sum w F_o^2]^{1/2}$ were 3.30% and 2.65%, respectively. The standard deviation of unit weight is 0.705. The final difference Fourier showed no peaks greater than $1.54 \text{ e}/\text{\AA}^3$.

The positional and anisotropic thermal parameters from the final least-squares refinement are given in Table 3, while the root-mean-square amplitudes of vibration are given in Table 4.

Bond distances and angles were calculated using DISMAT. The planarity of the COT rings and the dihedral angles between the planes were calculated using LSPLAN.

Figures 3 and 4 were drawn using ORTEPB1, a local version of C. K. Johnson's ORTEP plotting program.

The data used for the solution of the structure are presented in the Appendix. They are tabulated in columns of indices, F_o , standard deviation and $|F_o| - |F_c|$.

Table 3. Positional^a and thermal^b parameters.

NO.	ATOM	NEW X	NEW Y	NEW Z	NEW B11 OR B	NEW B22	NEW B33	NEW B12	NEW B13	NEW B23
1	NO1	.480632	.757446	.891578	2.561252	3.247394	3.847975	.384319	1.152794	.326488
2	NO2	.171854	.685705	.850253	2.952842	3.505543	3.533084	1.042100	1.151299	.377483
3	O1	.846734	.466625	.273545	3.921905	4.416336	4.473074	-.136771	1.414300	-.028615
4	O2	.814320	.484534	.051108	4.375747	4.586636	3.428346	-.448131	.449277	.490489
5	C1	.358128	.189394	.015156	.242777	13.434679	10.715089	-2.034628	2.201515	-9.982870
6	C2	.369673	.154942	.108402	9.359718	7.475897	9.494356	.506711	4.628319	-1.743845
7	C3	.402964	.194878	.193954	5.292918	10.174683	5.253514	3.106621	3.584870	1.392057
8	C4	.434279	.291274	.235055	1.673707	23.112695	3.308082	2.761251	-.438964	-4.045442
9	C5	.450959	.389212	.193321	5.213651	11.991734	20.293089	-4.799288	7.862652	-14.268747
10	C6	.445667	.416764	.105993	7.774388	6.219011	22.570365	2.742904	11.945522	4.927994
11	C7	.413604	.393251	.010428	10.288631	17.557631	21.778347	12.237881	12.505259	18.499147
12	C8	.377841	.215014	.473880	3.468758	21.875039	4.654351	-6.195133	3.161382	-3.765286
13	C9	.605674	.108618	.022707	4.032194	3.942835	5.208268	-.047215	1.489235	-.686155
14	C10	.617728	.065962	.116069	2.496064	2.766937	4.746623	.780609	.836366	1.076488
15	C11	.649869	.106190	.210192	1.738683	3.774674	4.190964	1.133392	-.325613	.154597
16	C12	.677764	.203899	.252585	1.475949	6.365917	3.641059	.246225	.929515	-.232159
17	C13	.681527	.307765	.215892	1.269021	4.037478	5.120958	.407999	.618454	-1.261840
18	C14	.652860	.357072	.118987	1.757077	2.946543	3.770786	.563739	.795024	.825701
19	C15	.642167	.314462	.026944	1.067447	3.960171	5.656338	-.143156	1.731144	.430659
20	C16	.616777	.211138	-.014149	3.352793	10.297917	1.641760	2.761283	.962788	1.151463
21	C17	.940336	.292271	.050541	4.810891	5.991993	4.025402	3.587633	3.978911	-.319336
22	C18	.874322	.283209	.515244	4.590373	7.778842	5.461030	-4.132736	-.196577	1.790187
23	C19	.834345	.138149	.049086	5.351014	4.823210	13.060180	.109027	4.690251	-3.399951
24	C20	.840897	.108063	.145694	8.410205	2.181577	18.182494	1.084628	9.459549	-.211054
25	C21	.898889	.141503	.247826	10.991160	9.196312	8.106034	9.405850	6.153009	7.069711
26	C22	.962872	.225557	.277871	5.543659	13.085595	5.981004	5.804934	-1.698614	-.926677
27	C23	-.006113	.298421	.229483	4.672689	9.917219	14.605983	.984655	4.221365	-3.368437
28	C24	.990616	.326285	.140797	7.347840	9.529574	8.884707	4.232877	6.208555	1.173779
29	C25	.217295	.050887	.233937	3.646921	3.735803	10.961730	.217966	2.358055	3.223567
30	C26	.169251	.140465	.167605	4.972478	4.043466	6.214067	.659287	-1.155703	3.502227
31	C27	.097971	.079457	.090392	8.778736	3.339050	5.483822	2.148244	2.626547	.380676
32	C28	.072942	-.008448	.146356	4.380164	6.014787	2.831393	.157467	-.692923	.937527
33	C29	.122120	.069999	.422734	4.306352	4.967903	9.500644	6.392973	-4.879278	-2.167241
34	C30	.152984	.150348	.501294	8.110392	4.671246	7.069761	.763342	1.900714	-3.224293
35	C31	.203140	.408526	.089891	6.040640	7.259593	6.646368	-3.753124	1.449718	-.851263
36	C32	.770727	.011569	.445091	4.730915	4.521552	.939042	1.092002	-.035729	.002493

^aIn fractional cell coordinates.^bThe complete temperature factor is $\exp(-1/4(a^*^2 B_{11} h^2 + b^*^2 B_{22} k^2 + c^*^2 B_{33} l^2 + 2a^* b^* B_{12} hk + 2a^* c^* B_{13} hl + 2b^* c^* B_{23} kl))$, where a*, b* and c* are the reciprocal cell dimensions.

Table 4. Root-mean-square amplitudes of vibration along the principal axes in units of Angstroms.

RMS DISPLACEMENTS IN UNITS OF ANGSTROMS						COMPARABLE B VALUES (ANGSTROM SQUARED)			
NO.	ATOM	RMS 1	RMS 2	RMS 3	AVE RMS	B (ISOTROPIC)	B11	B22	B33
1	ND1	.1725	.2023	.2248	.2010	3.19	2.35	3.23	3.99
2	ND2	.1645	.2089	.2344	.2046	3.31	2.14	3.45	4.34
3	O1	.2207	.2371	.2384	.2322	4.26	3.85	4.44	4.49
4	O2	.1986	.2281	.2700	.2341	4.33	3.11	4.11	5.76
THE TEMPERATURE FACTOR OF		C1 ARE NOT POSITIVE-DEFINITE.							
6	C2	.2591	.3378	.3712	.3261	8.40	5.30	9.01	10.88
7	C3	.1654	.2596	.3879	.2859	6.45	2.16	5.32	11.88
8	C4	.1254	.1924	.5608	.3499	9.67	1.24	2.92	24.83
9	C5	.1115	.1871	.6271	.3833	11.60	.98	2.76	31.05
10	C6	.1398	.2480	.5636	.3645	10.49	1.54	4.85	25.08
11	C7	.0843	.2059	.7155	.4326	14.78	.56	3.35	40.42
12	C8	.0895	.2246	.5519	.3479	9.55	.63	3.98	24.05
13	C9	.2142	.2254	.2653	.2360	4.40	3.62	4.01	5.56
14	C10	.1485	.2010	.2596	.2081	3.42	1.74	3.19	5.32
15	C11	.1172	.2256	.2647	.2119	3.55	1.08	4.02	5.53
16	C12	.1309	.2149	.2850	.2195	3.80	1.35	3.65	6.41
17	C13	.1212	.2017	.2833	.2128	3.58	1.16	3.21	6.36
18	C14	.1393	.1854	.2334	.1900	2.85	1.53	2.71	4.30
19	C15	.0854	.2216	.2702	.2077	3.41	.58	3.88	5.77
20	C16	.1367	.1757	.3777	.2532	5.06	1.48	2.44	11.27
21	C17	.1172	.2544	.3776	.2714	5.82	1.08	5.11	11.26
22	C18	.1471	.2399	.4042	.2843	6.38	1.71	4.54	12.90
23	C19	.1767	.2579	.4253	.3047	7.33	2.47	5.25	14.28
24	C20	.1375	.2357	.4927	.3252	8.35	1.49	4.39	19.17
25	C21	.0573	.2440	.5172	.3318	8.69	.26	4.70	21.12
26	C22	.1501	.3011	.4808	.3388	9.06	1.78	7.16	18.25
27	C23	.1792	.3311	.4577	.3422	9.24	2.53	8.66	16.54
28	C24	.1380	.3183	.4161	.3128	7.72	1.50	8.00	13.67
29	C25	.1736	.2114	.3970	.2783	6.12	2.38	3.53	12.44
30	C26	.1104	.2579	.3760	.2709	5.79	.96	5.25	11.16
31	C27	.1805	.2579	.3478	.2708	5.79	2.57	5.25	9.55
32	C28	.1548	.2707	.2955	.2480	4.86	1.89	5.79	6.89
THE TEMPERATURE FACTOR OF		C29 ARE NOT POSITIVE-DEFINITE.							
34	C30	.1646	.3110	.3643	.2924	6.75	2.14	7.64	10.48
35	C31	.1897	.2972	.3659	.2934	6.79	2.84	6.97	10.57
36	C32	.1072	.2179	.2808	.2143	3.63	.91	3.75	6.23

RESULTS AND DISCUSSION

Physical Properties of $[\text{Ln}(\text{COT})(\text{THF})_2][\text{Ln}(\text{COT})_2]$ Compounds

$[\text{La}(\text{COT})(\text{THF})_2][\text{La}(\text{COT})_2]$ and $[\text{Nd}(\text{COT})(\text{THF})_2][\text{Nd}(\text{COT})_2]$ have similar physical properties. The gold La and the bright green Nd crystalline solids both readily lose THF at room temperature under high vacuum and further decompose when heated under vacuum to 85°C. Both are insoluble in nonpolar solvents but are sparingly soluble in THF. The maximum solubility of $[\text{Nd}(\text{COT})(\text{THF})_2][\text{Nd}(\text{COT})_2]$ has been estimated to be 0.5 millimole per liter from a visible spectrum using Beer's Law. This was calculated from observed maximum absorbance of 0.007 of the 585 nm Nd^{3+} band assuming the molar extinction coefficient to be 7 l/cm-mole.

Analytical Results

Commercial analyses were unsatisfactory. Analyses were done in the manner described in the experimental section. Reasonable agreement with calculated values were found for $[\text{La}(\text{COT})(\text{THF})_2][\text{La}(\text{COT})_2]$, $[\text{Nd}(\text{COT})(\text{THF})_2][\text{Nd}(\text{COT})_2]$ and $\text{Nd}_2(\text{COT})_3$, Table 1. Because of the procedures involved, confidence limits are set at about 0.5% for the metal, 2% for the THF and 2% for COT^{2-} if hydrolysis was complete. The total composition of

$[\text{Nd}(\text{COT})(\text{THF})_2][\text{Nd}(\text{COT})_2]$ however has been established by an X-ray structure determination.

Structure of $[\text{Nd}(\text{COT})(\text{THF})_2][\text{Nd}(\text{COT})_2]$

The molecular structure consists of an ion pair composed of an $[\text{Nd}(\text{COT})_2]^-$ anion and a $[\text{Nd}(\text{COT})(\text{THF})_2]^+$ cation as shown in Figure 3. Thus, the compound is named cyclooctatetraenylbis(tetrahydrofuran)neodymium(III) bis(cyclooctatetraenyl)neodymate(III). The anion is composed of Nd1 and COT rings 1 and 2. The atoms in ring 1 are numbered C1-C8, while those in ring 2 are numbered C9-C16. Ring 1 is the terminal COT, while ring 2 is located between the neodymiums. The cation is composed of Nd2, COT ring 3 and two THF rings. The atoms in ring 3 are numbered C17-C24. The atoms in the first THF ring are numbered O1 and C25-C28, while the atoms in the second THF ring are numbered O2 and C29-C32.

The average C-C bond lengths in rings 1, 2 and 3 are 1.38 (6), 1.42 (1) and 1.41 (2) Å, respectively, Table 5. These distances are within experimental error of the 1.39 Å average C-C bond length found in $[\text{K}(\text{diglyme})][\text{Ce}(\text{COT})_2]$, $\text{U}(\text{COT})_2$ and $[\text{Ce}(\text{COT})\text{Cl} \cdot 2\text{THF}]_2$ [25, 26, 30]. The average angles in rings 1, 2 and 3 are 134.8 (2.3), 134.9 (0.7) and 134.9 (1.5) Å, respectively, Table 5. These angles are well within experimental error of the 135° angles of a regular planar octagon.

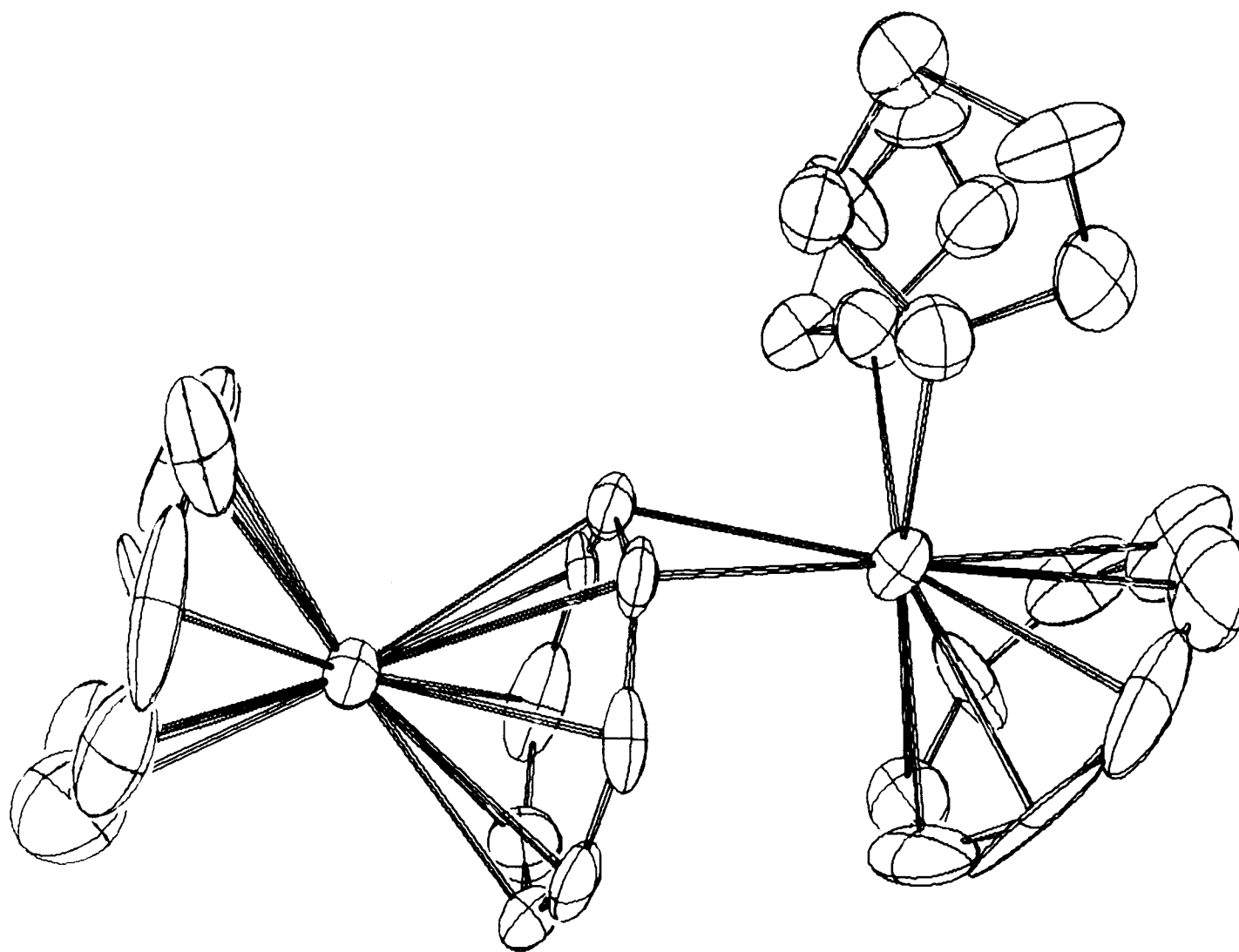


Figure 3. A perspective view of $[\text{Nd}(\text{COT})(\text{THF})_2][\text{Nd}(\text{COT})_2]$. Thermal ellipsoids are drawn at the 50% probability contour.

Table 5. Bond lengths and angles in cyclooctatetraene rings.

Bond	Length, Å	Group	Angle, deg.
C1-C2	1.364(48)	C8-C1-C2	134.39(4.76)
C2-C3	1.280(41)	C1-C2-C3	133.99(5.37)
C3-C4	1.392(48)	C2-C3-C4	138.29(4.77)
C4-C5	1.453(52)	C3-C4-C5	133.03(4.83)
C5-C6	1.279(57)	C4-C5-C6	132.90(6.58)
C6-C7	1.337(59)	C5-C6-C7	145.50(5.99)
C7-C8	1.530(57)	C6-C7-C8	122.51(5.52)
C8-C1	1.441(49)	C7-C8-C1	137.74(4.15)
Average ^a	1.384(57)		134.79(2.29)
C9-C10	1.404(30)	C16-C9-C10	134.99(2.19)
C10-C11	1.382(28)	C9-C10-C11	133.01(2.25)
C11-C12	1.401(29)	C10-C11-C12	136.52(2.09)
C12-C13	1.437(29)	C11-C12-C13	135.35(2.13)
C13-C14	1.467(28)	C12-C13-C14	136.38(2.08)
C14-C15	1.367(28)	C13-C14-C15	131.05(2.29)
C15-C16	1.452(31)	C14-C15-C16	134.78(2.03)
C16-C9	1.447(32)	C15-C16-C9	136.81(2.31)
Average ^a	1.419(14)		134.86(0.69)
C17-C18	1.427(36)	C24-C17-C18	135.82(2.59)
C18-C19	1.378(39)	C17-C18-C19	140.57(3.11)
C19-C20	1.410(48)	C18-C19-C20	130.84(2.97)
C20-C21	1.533(54)	C19-C20-C21	133.63(4.26)
C21-C22	1.476(48)	C20-C21-C22	130.86(5.15)
C22-C23	1.360(49)	C21-C22-C23	134.96(5.12)
C23-C24	1.307(49)	C22-C23-C24	141.45(5.24)
C24-C17	1.367(39)	C23-C24-C17	131.11(3.88)
Average ^a	1.407(25)		134.90(1.49)

^aStandard deviations for the mean values for this and all subsequent tables were calculated from the variance using the equations $\sigma^2 = (\sum_{i=1}^n (x_i - \bar{x})^2) / (n-1)$ and $\sigma_{\bar{x}} = \sigma / (n)^{1/2}$ where σ^2 is the standard deviation of an individual observation and $\sigma_{\bar{x}}$ is the standard deviation of the mean.

The atoms in rings 1, 2 and 3 average 0.034, 0.048 and 0.026 Å from their respective least-squares planes, Table 6. The planarity of the rings, the bond distances and the angles demonstrate the aromatic nature of the ten π -electron dianion in this structure.

Table 6. Least-squares planes of cyclooctatetraene rings.

Ring 1		Ring 2		Ring 3	
Atom	Distance ^a	Atom	Distance ^a	Atom	Distance ^a
C1	-.02275	C9	-.01286	C17	-.02404
C2	-.00985	C10	-.05568	C18	.02671
C3	.04746	C11	.01252	C19	.01155
C4	-.02107	C12	.05814	C20	.02069
C5	-.04144	C13	-.00847	C21	-.02996
C6	.05433	C14	-.07662	C22	-.00316
C7	-.01948	C15	.03950	C23	.04142
C8	.01280	C16	.04346	C24	-.02011
Average	.03489		.04810		.02640
<u>Parameters from Equations of Plane^b</u>					
A	15.638	A	16.296	A	-12.477
B	-4.321	B	-2.559	B	8.464
C	-3.404	C	-3.744	C	3.811
D	4.753	D	9.519	D	-9.042
<u>Angles Between Planes^c</u>					
1-2	8.25°	1-3	-22.34°	2-3	-30.29°

^aDistances in Angstroms of individual atoms from least-squares plane.

^bEquation for least-squares plane in monoclinic coordinates of the form $Ax + By + Cz + D = 0$.

^cNegative values for angles involving plane 3 are a result of the form of the direction cosines of the normals to the planes.

In the anion, ring 1 is symmetrically bonded to Nd1 with an average Nd-C distance of 2.66 (2) Å, Table 7. This distance is in good agreement with an estimated distance of 2.69 Å. This estimate was calculated by the method used by Raymond and coworkers [30]. This method accurately estimated the Th-C and Ce-C bond lengths in Th(COT)₂ and [K(diglyme)][Ce(COT)₂] by adding the difference between ionic radii of the metals and U⁴⁺ to the average U-C bond length in U(COT)₂. The difference between Nd³⁺, 1.09 Å, and U⁴⁺, 1.05 Å, is 0.04 Å [37]. The average U-C bond length in U(COT)₂ is 2.65 Å [30].

Table 7. Neodymium-carbon distances.

Ring 1	Distance, Å	Ring 2	Distance, Å
Nd1-C1	2.673(22)	Nd1-C9	2.768(22)
Nd1-C2	2.734(34)	Nd1-C10	2.770(19)
Nd1-C3	2.681(27)	Nd1-C11	2.801(18)
Nd1-C4	2.717(28)	Nd1-C12	2.821(20)
Nd1-C5	2.683(32)	Nd1-C13	2.771(19)
Nd1-C6	2.537(38)	Nd1-C14	2.765(19)
Nd1-C7	2.681(36)	Nd1-C15	2.820(19)
Nd1-C8	2.577(28)	Nd1-C16	2.784(21)
Average	2.660(24)	Average	2.787(19)
Ring 3	Distance, Å	Ring 2	Distance, Å
Nd2-C17	2.708(24)	Nd2-C14	2.700(18)
Nd2-C18	2.616(23)	Nd2-C13	2.896(20)
Nd2-C19	2.696(28)	Nd2-C15	3.029(19)
Nd2-C20	2.649(27)	Nd2-C12	3.59
Nd2-C21	2.679(22)	Nd2-C16	3.78
Nd2-C22	2.653(26)	Nd2-C11	4.28
Nd2-C23	2.633(31)	Nd2-C9	4.42
Nd2-C24	2.756(27)	Nd2-C10	4.67
Average	2.673(16)		

Ring 2 is symmetrically bonded to Nd1 but unsymmetrically located with respect to Nd2, Table 7. The average Nd1-C distance is 2.79 (2) Å. This distance is a full 0.1 Å longer than the expected value. C14, C13 and C15 are also in close proximity to Nd2 with Nd2-C distances of 2.70 (2), 2.90 (2) and 3.03 (3) Å, respectively. In fact, C14 is closer to Nd2, 2.70 (2) Å, than to Nd1, 2.76 (2) Å. Furthermore, although the carbon atoms are in a very nearly eclipsed configuration, the planes of rings 1 and 2 are not parallel, but rather intersect at an angle of 8.25°. This tilt causes the C_n-C_{n+8} distances to range from 3.75 to 4.22 Å.

The position of ring 2 in [Nd(COT)(THF)₂][Nd(COT)₂] is unique for all known lanthanide and actinide COT compounds. Its position makes it the first example of a lanthanide or actinide asymmetric M(COT)₂ unit. Its position relative to Nd2 is the first example of a lanthanide or actinide asymmetrically bonded to a COT ring.

In the cation, ring 3 is symmetrically bonded to Nd2 with an average bond length of 2.67 (2) Å, Table 7. The plane of ring 3 intersects the plane of ring 1 at an angle of 22.34° and the plane of ring 2 at an angle of 30.29°.

The Nd2-C14 distance, 2.70 (2) Å, implies a bonding interaction. This distance is 0.2-0.4 Å longer than expected for a Nd-C σ-bond based on the assumption that the difference between a Nd-C σ-bond and a U-C σ-bond would be small. U-C σ-bonds range from 2.33 to

2.5 Å [38]. The observed distance is that expected for a normal π -bond between Nd^{3+} and a COT^{2-} ring (vide supra). Clearly, however, the Nd2-C14 interaction can not be a normal π -bond, because there are no other Nd2-ring 2 distances of comparable length. The next closest distance found is Nd2-C13, 2.90 (2) Å.

This interaction can be explained by electrostatic and steric arguments. Assuming purely ionic bonding, the positive charge of the cation is centered on Nd2 while the negative charge of the anion will be shared by rings 1 and 2. Therefore an interaction between Nd2 and ring 2 is expected. But because Nd2 is already coordinated to ring 3 and the two THF oxygens, there is only room for part of ring 2 in its coordination sphere. In particular, C14 is definitely in the coordination sphere of Nd2 and C13 and C15 may well be.

Using the arguments just given, one can explain the longer than expected Nd1-ring 2 distance. The effective negative charge of ring 2 has been reduced with respect to ring 1, and therefore, is not as strongly attracted to Nd1 as is ring 1. Also the asymmetry of Nd2 with respect to ring 2, causes rings 1 and 2 to be nonparallel.

The dihedral angles between the planes of the rings is then a consequence of the coordination about Nd2. This is particularly noticeable for the angles involving ring 3. Ring 3 is forced into its configuration because the THF oxygen atoms occupy coordination sites.

Other interesting features are noted in comparing the three COT rings. Values of the standard deviation of bond lengths and angles, Table 5, thermal parameters, Table 3, and root-mean-square amplitudes of vibration, Table 4, are much less for ring 2 than for rings 1 and 3. Average standard deviations of the bond lengths and angles in ring 2 are 0.014 \AA and 0.69° while in rings 1 and 3 they are 0.057 \AA and 2.29° and 0.025 \AA and 1.49° , respectively. Thermal parameters for ring 2 are only about one half as large as the corresponding parameters for rings 1 and 3. The root-mean-square amplitudes of vibration for ring 2 are 0.137 , 0.206 and 0.280 \AA while in rings 1 and 3 they are 0.139 , 0.236 and 0.540 \AA and 0.138 , 0.273 and 0.446 \AA , respectively. These data clearly show that ring 2 is much more rigidly fixed in space than are rings 1 and 3. This does not seem surprising when one considers that ring 2 interacts with both Nd1 and Nd2 while rings 1 and 3 are bonded to only one Nd.

The observed Nd1-ring 2 bond lengthening and the root-mean-square data for $[\text{Nd}(\text{COT})(\text{THF})_2][\text{Nd}(\text{COT})_2]$ are the opposite of the data observed by Hodgson and Raymond for $[\text{K}(\text{diglyme})][\text{Ce}(\text{COT})_2]$ [25]. In the latter, even though ring 2 is coordinated to both Ce and K, there is no difference in the Ce-C bond length and ring 2 exhibits vibrational amplitudes twice as large as ring 1. These differences may be accounted for by differences in molecular geometries. We observe that ring 2 is asymmetrically located with respect to the

cation and although rings 1 and 2 are essentially eclipsed they are not parallel. Hodgson and Raymond observed that their ring 2 is symmetrically coordinated to their cation and that rings 1 and 2 are staggered and parallel. It would seem then that small differences in energy cause the differences in M-C bond lengths and vibrational amplitudes of the molecules and that the configuration the molecules assumes in the crystal may be determined by packing considerations.

The bond lengths and angles for the THF rings, Table 8, are in good agreement with those found in $[\text{Ce}(\text{COT})\text{Cl} \cdot 2\text{THF}]_2$ [26]. The oxygen atom of both rings is coordinated to Nd2. The Nd2-01 and Nd2-02 distances are 2.59 (1) and 2.57 (1) Å, respectively. The 01-Nd2-02 angle is 73.22 (0.47)° and the 01-02 distance is 3.073 Å.

The intramolecular Nd1-Nd2 distance is 5.07 Å.

Table 8. Bond lengths and angles for tetrahydrofuran rings.

Bond	Length, Å	Group	Angle, deg.
01-C25	1.495(24)	C28-01-C25	110.16(1.95)
C25-C26	1.538(28)	01-C25-C26	105.98(1.57)
C26-C27	1.548(31)	C25-C26-C27	101.19(1.85)
C27-C28	1.521(30)	C26-C27-C28	105.59(1.83)
C28-01	1.486(22)	C27-C28-01	103.60(1.56)
02-C29	1.482(22)	C32-02-C29	108.20(2.33)
C29-C30	1.489(30)	02-C29-C30	105.83(1.61)
C30-C31	1.482(33)	C29-C30-C31	105.16(2.25)
C31-C32	1.522(30)	C30-C31-C32	107.30(2.02)
C32-02	1.461(20)	C31-C32-02	105.96(1.56)
Nd2-01	2.587(14)	01-Nd2-02	73.22(0.47)
Nd2-02	2.566(14)		

The crystal structure consists of four anion-cation pairs per unit cell, Figure 4. The anions lie very close to the glide planes at $y = 0.25$ and $y = 0.75$ with $y(\text{Nd1}) = 0.243, 0.757, 0.743$ and 0.257 , and very close to the (200) plane with $x(\text{Nd1}) = 0.519, 0.481, 0.481$ and 0.519 , with the ring-Nd1-ring axis in x-direction. The cations are located on the ends of the anion extending almost to the (100) plane. This packing arrangement gives an overall layer lattice type structure.

Structure of $[\text{La}(\text{COT})(\text{THF})_2][\text{La}(\text{COT})_2]$

Because the infrared spectrum, chemical properties (vide infra) and observed density, 1.76 g/cm^3 , of $[\text{La}(\text{COT})(\text{THF})_2][\text{La}(\text{COT})_2]$ are virtually identical with those of $[\text{Nd}(\text{COT})(\text{THF})_2][\text{Nd}(\text{COT})_2]$, the crystals are expected to be isomorphous. Examination of crystals of $[\text{La}(\text{COT})(\text{THF})_2][\text{La}(\text{COT})_2]$ under a microscope also revealed that they have the same needlelike shape. No crystals were large enough however to do a single crystal X-ray determination. Unfortunately X-ray powder patterns were not sharp and only five lines were of suitable quality to be measured accurately. Therefore there is not enough data to lead to a definite conclusion.

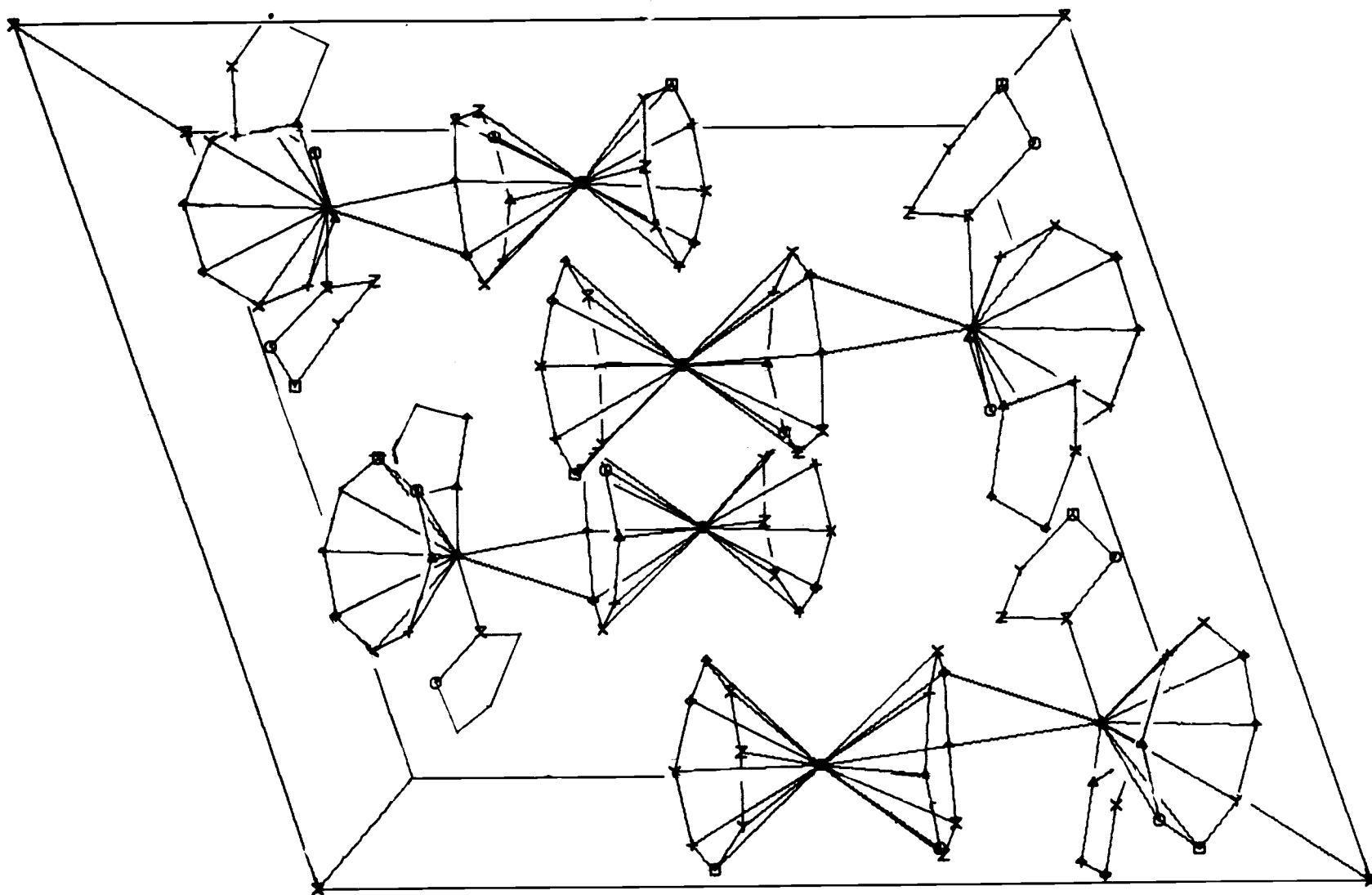


Figure 4. A perspective view of the packing of $[\text{Nd}(\text{COT})(\text{THF})_2][\text{Nd}(\text{COT})_2]$ as viewed down the b -axis. The origin of the cell is in the lower left front corner.

Infrared Spectra

The infrared spectra of $[\text{La}(\text{COT})(\text{THF})_2][\text{La}(\text{COT})_2]$, $[\text{Nd}(\text{COT})(\text{THF})_2][\text{Nd}(\text{COT})_2]$ and $\text{Nd}_2(\text{COT})_3$ are presented and compared with similar compounds in Table 9. By analogy the bands centered at 3000, 893 and 685 cm^{-1} are assigned to the C-H stretching, C-H (\parallel) bending and the C-H (\perp) bending fundamentals of the planar D_{8h} COT^{2-} rings. The 2973, 1010 and 860 cm^{-1} bands are assigned to the C-H stretching, C-O stretching and C-H bending fundamentals of the THF rings. Additional bands appearing in the spectra presumably arise from changes in effective site symmetry in the COT^{2-} rings and infrared active molecular fundamentals.

Raman Spectra

The Raman spectrum of a polycrystalline sample of $[\text{Nd}(\text{COT})(\text{THF})_2][\text{Nd}(\text{COT})_2]$ consists of two strong bands at 750 and 242 cm^{-1} and a complex region from $350\text{--}500\text{ cm}^{-1}$, as shown in Figure 5. The 750 cm^{-1} band is assigned as the symmetric breathing mode of the COT^{2-} rings and is identical to the 750 cm^{-1} band observed from $\text{U}(\text{COT})_2$ and $\text{K}[\text{Ce}(\text{COT})_2]$ [13]. The 242 cm^{-1} band is substantially higher in frequency than the lowest frequency bands observed for $\text{U}(\text{COT})_2$, 215 cm^{-1} , and $\text{K}[\text{Ce}(\text{COT})_2]$, 200 cm^{-1} [13]. In addition the $350\text{--}500\text{ cm}^{-1}$ region is considerably more complex

Table 9. Infrared spectra of COT compounds.^a

(1)	(2)	(3)	(4) ^b	(5) ^b	(6) ^c
3004 (m)	3003 (m)	3000 (m)			2994 (m)
2982 (m)	2973 (m)				
2925 (w)	2920 (w)	2921 (m)			
2875 (w)	2886 (m)				
	2861 (m)				
			1060 (w)		
1019 (s)	1010 (s)		1010 (s)		
			923 (w)		
894 (s)	893 (s)	894 (s)	880 (s, split)	890 (s)	880 (s)
861 (s)	862 (s)				
832 (m)	832 (m)				
	780 (m)	798 (m)	801 (w)	810 (s)	
		771 (m)		795 (s)	
736 (m)	741 (m)	744 (s)	745 (m)	770 (m)	
			716 (w, sh)	730 (ms)	
709 (sh)	710 (sh)		705 (sh)	715 (m)	
688 (vs)	688 (vs)	685 (vs)	697 (vs)	670 (s)	684 (s)

(1) = [La(COT)(THF)₂][La(COT)₂].

(2) = [Nd(COT)(THF)₂][Nd(COT)₂].

(3) = Nd₂(COT)₃.

(4) = [Nd(COT)Cl₂ · 2THF]₂.

(5) = KNd(COT)₂.

(6) = COT²⁻.

^avs = very strong, s = strong, m = medium, w = weak, sh = shoulder.

^bSee reference [13]. ^cSee reference [41].

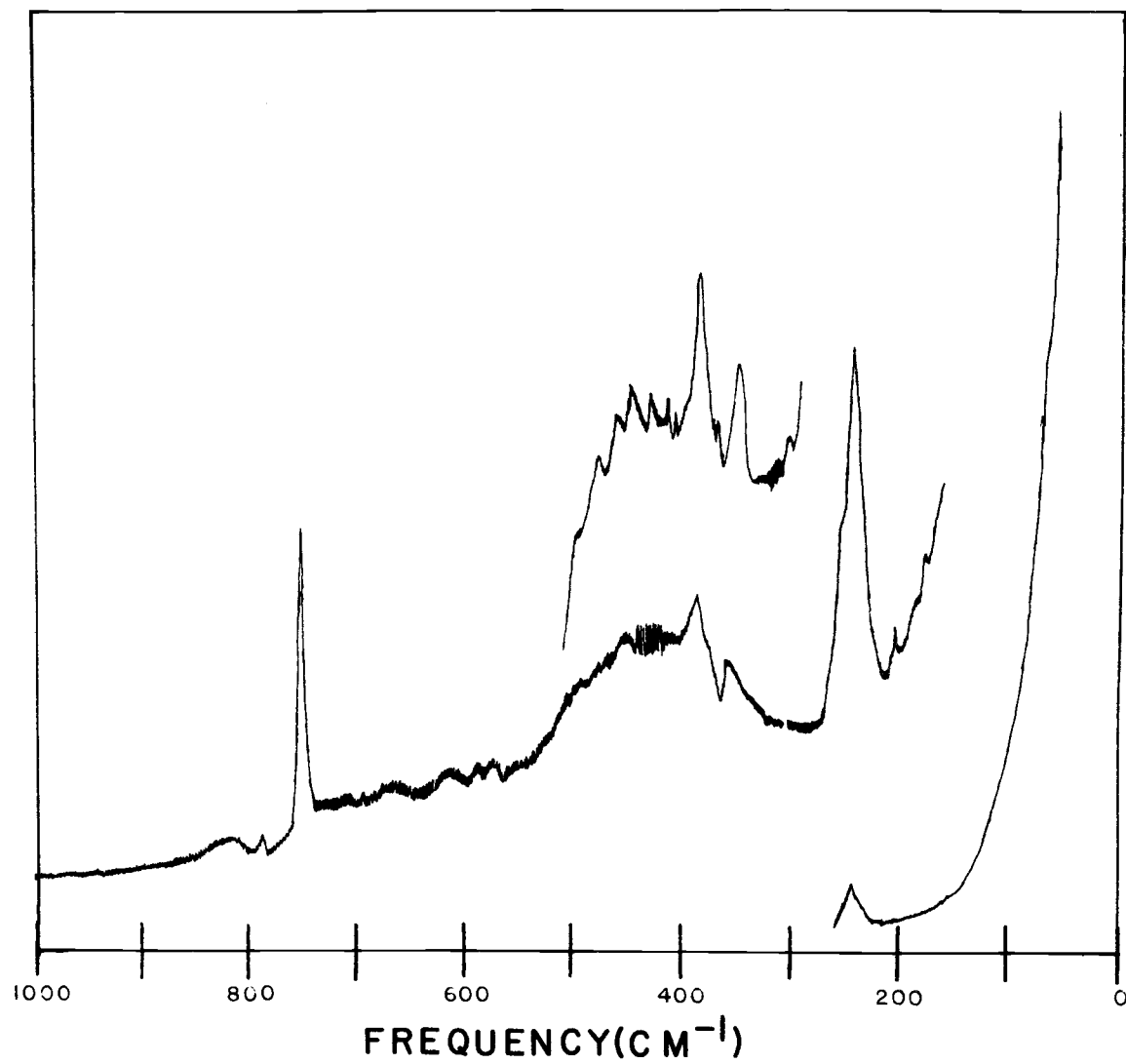


Figure 5. Raman spectrum of $[\text{Nd}(\text{COT})(\text{THF})_2][\text{Nd}(\text{COT})_2]$.

than that observed for the above two compounds. We suggest the above differences are due to the molecular asymmetry of $[\text{Nd}(\text{COT})(\text{THF})_2][\text{Nd}(\text{COT})_2]$. This asymmetry will induce a mixing of the symmetric and antisymmetric ring-metal stretching modes. This mixing is expected to increase the frequency of the symmetric mode because the antisymmetric mode lies above the symmetric modes as for example, in the classic sandwich molecule, ferrocene, where the symmetric ring-metal stretch is observed at 303 cm^{-1} while the antisymmetric ring-metal stretch is observed at 478 cm^{-1} [39]. This mixing also produces a higher frequency Raman active Nd-ring stretch which contributes to the complexity of the $350\text{-}500\text{ cm}^{-1}$ region. This region is further complicated by COT^{2-} ring bending and Nd-O stretching modes.

No Raman spectrum of $[\text{La}(\text{COT})(\text{THF})_2][\text{La}(\text{COT})_2]$ was observed because of fluorescence.

Nuclear Magnetic Resonance

Repeated attempts to observe the proton magnetic resonance spectrum of $[\text{Nd}(\text{COT})(\text{THF})_2][\text{Nd}(\text{COT})_2]$ proved fruitless. This was attributed to two causes. The estimated solubility, maximum of 0.5 mmol/L , makes the observation difficult. In addition, the paramagnetism of the sample is expected to broaden the lines and make their observation more difficult.

To overcome the problem of paramagnetism, $[\text{La}(\text{COT})(\text{THF})_2][\text{La}(\text{COT})_2]$ was prepared. However its low solubility still precluded observation of its proton magnetic resonance spectrum.

Magnetic Susceptibility

The magnetic moment of $[\text{Nd}(\text{COT})(\text{THF})_2][\text{Nd}(\text{COT})_2]$ at 16° C is 3.20 B.M. This moment compares well with the moments observed in $[\text{Nd}(\text{COT})\text{Cl} \cdot 2\text{THF}]_2$, 3.37 B.M., and $\text{KNd}(\text{COT})_2$, 2.98 B.M. [13]. The moment observed in $\text{Nd}(\text{SO}_4)_3 \cdot 8\text{H}_2\text{O}$ is 3.52 [40]. Thus the neodymium is in a formal oxidation state of +3 as expected.

Chemical Properties and Reactions

The most prominent property of the COT compounds is their extreme sensitivity to air and moisture. Trace quantities of oxygen and H_2O cause decomposition. On standing in open vessels in an inert atmosphere box whose maximum O_2 concentration was 8 ppm, the compounds turned red within 20 minutes. On exposure to air they spontaneously inflame, often leaving only an Ln_2O_3 colored powder.

Thermal Decomposition

Both $[\text{La}(\text{COT})(\text{THF})_2][\text{La}(\text{COT})_2]$ and $[\text{Nd}(\text{COT})(\text{THF})_2][\text{Nd}(\text{COT})_2]$ are thermally unstable. While pumping on a sample of the latter at 25° C at 10^{-4} mm Hg, the green crystals

lose all their THF within three hours and become a gold powder. The gold solid satisfactorily analyzes for $\text{Nd}_2(\text{COT})_3$.

Warming to 85°C causes further decomposition. Volatile products identified were COT, cyclooctatrienes and benzene. The nonvolatile residue was not characterized.

Hydrolysis

Two ml of degassed H_2O was vacuum transferred onto weighed samples of $[\text{Ln}(\text{COT})(\text{THF})_2][\text{Ln}(\text{COT})_2]$. If the mixture is allowed to warm too rapidly a red solid is formed and hydrolysis is incomplete. Careful warming of the mixture affords complete hydrolysis and produces a white insoluble powder, presumably $\text{Ln}(\text{OH})_3$, THF and cyclooctatrienes. The trienes were identified by extracting the yellow organic layer into CCl_4 and obtaining an pmr spectrum. The spectrum showed a broad singlet at $\delta = 2.4$ (methylene H's) and a complex multiplet at about $\delta = 5.9$ (methine H's) with area ratios of 4:6. THF was also observed.

Oxidation

Oxidations of $\text{Nd}_2(\text{COT})_3$ and $[\text{Nd}(\text{COT})(\text{THF})_2][\text{Nd}(\text{COT})_2]$ using O_2 and/or air were done. In all cases COT^{2-} was oxidized to COT in about 40% yield. The other product was a red solid, which was not characterized. Its infrared spectrum, however,

indicated the presence of C-H stretching and the complete absence of COT^{2-} .

Reaction with UCl_4

Treatment of solid $[\text{Ln}(\text{COT})(\text{THF})_2][\text{Ln}(\text{COT})_2]$ with a solution of UCl_4 in THF produced $\text{U}(\text{COT})_2$ which was characterized by its visible spectrum. Unlike the reactions of $\text{KLn}(\text{COT})_2$ with UCl_4 [13], reaction was not instantaneous, but rather took 20-30 minutes to complete. This difference in reactivity is attributed to the low solubility of $[\text{Ln}(\text{COT})(\text{THF})_2][\text{Ln}(\text{COT})_2]$ and does not suggest that they are more stable than $\text{KLn}(\text{COT})_2$.

CONCLUSIONS

Neodymium, lanthanum and erbium metal atoms react with cyclooctatetraene at -196°C to form a new class of lanthanide COT compounds, $\text{Ln}_2(\text{COT})_3$. These compounds are extremely air and moisture sensitive, are insoluble in nonpolar solvents but are sparingly soluble in THF.

The neodymium and lanthanum compounds crystalize from THF with two solvent molecules. The molecular composition was established by metal analysis and chemical decomposition. Physical and chemical evidence are consistent with ionic bonding.

Finally, a complete single crystal X-ray determination of the neodymium compound shows that the molecule is an anion-cation pair where the anion is $[\text{Nd}(\text{COT})_2]^-$ and the cation is $[\text{Nd}(\text{COT})(\text{THF})_2]^+$. The COT rings demonstrate the aromatic nature of a ten π -electron dianion, but the asymmetric location of Nd2 with respect to ring 2 and the nonparallel configuration of the COT rings make the molecular geometry unlike that of any previously reported lanthanide or actinide COT compounds.

PART II

THE REACTIONS OF NEODYMIUM AND ERBRIUM CHLORIDES WITH THE DICARBOLLIDE ION

INTRODUCTION

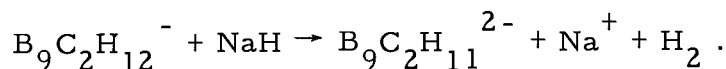
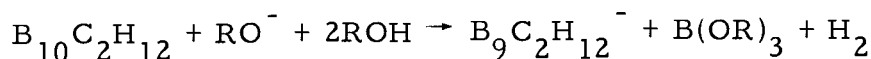
Part I of this thesis dealt with the preparation and properties of π -carbocyclic lanthanide compounds where the π -system is the ten π -electron cyclooctatetraene dianion. Part II deals with the preparation and properties of lanthanide compounds with a second type of π -ligand system, the six π -electron dicarbollide ion, $B_9C_2H_{11}^{2-}$.

The reasons for working with the dicarbollide ion were twofold. First, no lanthanide carboranes of any type have been reported. Second, the dicarbollide ion behaves very similarly to the cyclopentadienide ion, Cp^- , in its reactions with d-transition metal halides (vide infra). This similarity suggested that perhaps the $B_9C_2H_{11}^{2-}$ analogs of the lanthanide cyclopentadienides could be prepared.

In 1963 carboranes with the formula $B_{10}C_2H_{10}R_2$ were first prepared by reacting decaborane(14), $B_{10}H_{14}$, with acetylenic compounds in the presence of Lewis bases [42]. The structure of the parent compound, $R=H$, commonly referred to as ortho-carborane, was shown [43] to have a regular icosahedral geometry with the two carbon atoms at adjacent vertices numbered 1 and 2. The other possible $B_{10}C_2H_{12}$ isomers, the 1,7- and 1,12-derivatives, commonly called meta- and para-carborane, respectively, can be prepared by thermal rearrangements of the 1,2-isomer. The nomenclature used for these and other carboranes is in accordance with the

rules set forth by Adams [44].

The dicarbollide ion, (3)-1,2-dicarbaundecahydro-nido-undecaborate(2-), can be prepared in a two step synthesis from ortho-carborane, 1,2-dicarba-closo-dodecacarborane(12), according to the equations



The selective base degradation [45] of carborane removes the number 3 boron to give $\text{B}_9\text{C}_2\text{H}_{12}^-$, (3)-1,2-dicarbado-dodecahydro-nido-undecaborate(-). This in turn is treated with NaH in THF [46].

A drawing of the dicarbollide ion showing approximately sp^3 hybrid orbitals directed at the vacant 3 position is shown in Figure 6. These orbitals were derived from Moore, Lohr and Lipscomb's calculation of a molecular orbital scheme for $\text{B}_{11}\text{H}_{11}^{2-}$ [47]. This scheme applies equally well to the hypothetical $\text{B}_{11}\text{H}_{11}^{4-}$ which is isoelectronic with $\text{B}_9\text{C}_2\text{H}_{11}^{2-}$. Six electrons are left in five orbitals directed toward the vacant 3 position. In $\text{B}_{11}\text{H}_{11}^{4-}$ the six electrons would occupy a strongly bonding A_1 orbital and two degenerate bonding E_1 orbitals, leaving two degenerate strongly antibonding E_2 orbitals vacant. These molecular orbitals are generated from the five atomic sp^3 orbitals present in the open face and are similar to

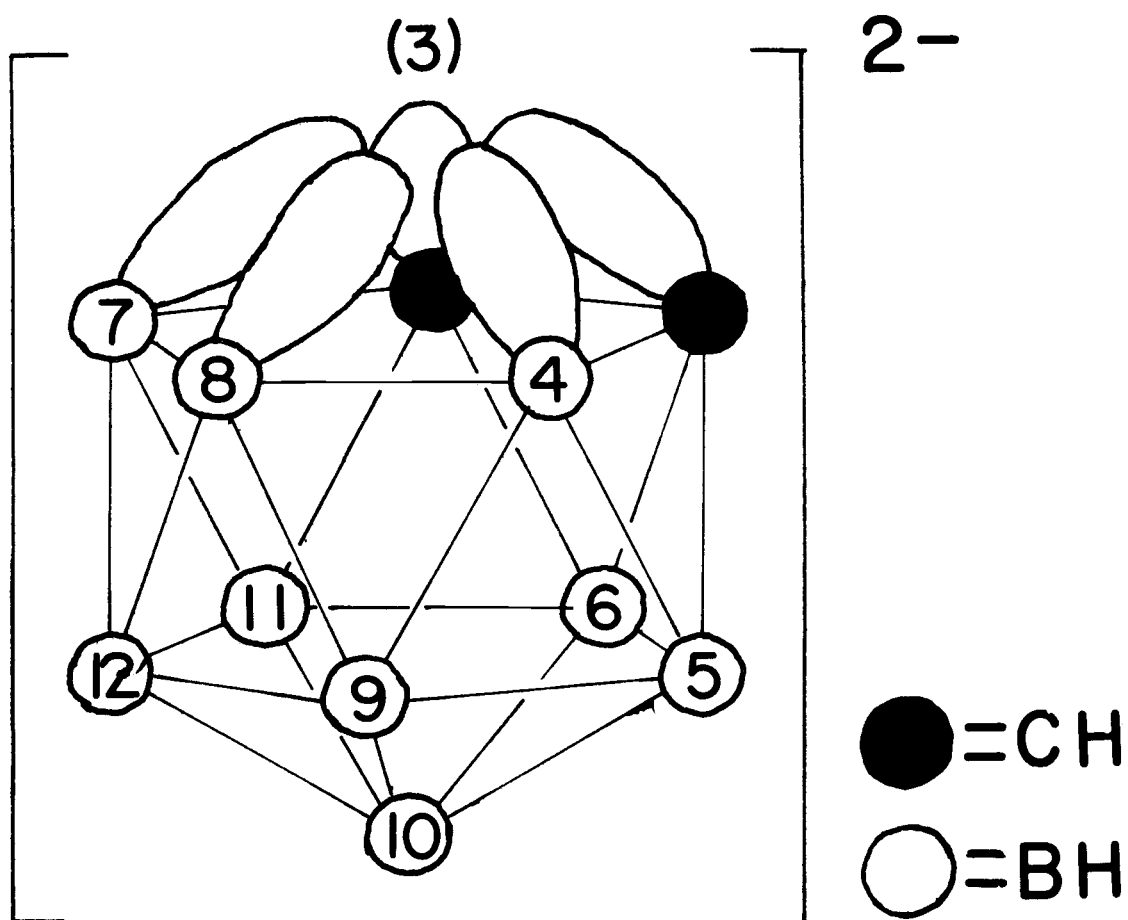


Figure 6. A schematic drawing of (3)-1, 2- $\text{B}_9\text{C}_2\text{H}_{11}^{2-}$, the dicarbollide ion, showing approximately sp^3 hybrid orbitals directed at the vacant (3)-vertex.

those orbitals in the cyclopentadienide ion, Cp^- . In the case of $\text{B}_9\text{C}_2\text{H}_{11}^{2-}$ the exact degeneracy of the E orbitals would be removed, but this should not affect their energies greatly, and one might expect $\text{B}_9\text{C}_2\text{H}_{11}^{2-}$ to resemble Cp^- in its reactions with transition metal halides.

The first experimental test of this hypothesis came in 1965 when Hawthorne, Young and Wegner prepared the dicarbollide analog of ferrocene, $[\text{Fe}(\text{B}_9\text{C}_2\text{H}_{11})_2]^{2-}$ [48]. The sandwich structure was confirmed by X-ray diffraction studies [49]. This discovery enormously broadened the scope of boron chemistry. In the next few years Hawthorne and coworkers prepared a variety of similar complexes involving Cr, Mo, W, Mn, Re, Fe, Co, Ni, Pd, Cu and Au [50]. Of these the Cu and Au compounds have no Cp^- analogs. The attempted preparation of an Ag dicarbollide complex proved fruitless [51]. Other carboranes of these metals [50, 52, 53, 54] as well as Zn [55], Pt [56], Ti, Zr and V [57, 58] have been reported.

Recent interest has centered on the Group VIII B metals. $\text{HRh}(\text{PPh}_3)_2(\text{B}_9\text{C}_2\text{H}_{11})$ has been prepared and has been shown to catalyze isomerization and hydrogenation of olefins [59] and to selectively catalyze deuterium exchange in B-H bonds [60]. The mechanism for the latter reaction is believed to involve an oxidative addition of a terminal B-H bond to the Rh complex. Support for this mechanism comes from correlations of reactivity patterns with

patterns of nucleophilic substitution and from the isolation of two Ir carboranes in which a B-H bond has oxidatively added to the Ir [61, 62]. A Ru dicarbollide has also been prepared [63].

NdCl_3 and ErCl_3 were selected as the chlorides to investigate so as to observe possible differences in product formation or reactivity between a light and a heavy lanthanide due to the lanthanide contraction. As mentioned in the Introduction in Part I, one consequence of this contraction is a difference in the products of the reactions of NaCp with LnCl_3 [22, 23]. These products are only LnCp_3 with light lanthanides but are LnCp_3 , LnCp_2Cl and LnCpCl_2 with heavy lanthanides. A second consequence of this contraction is that the coordination number of the metal decreases in going from compounds of the light to heavy lanthanides. For example, Nd^{3+} is nine coordinate in NdCl_3 [64], but Er^{3+} is only eight coordinate in ErCl_3 [65].

The present work shows there are striking differences in the types of products obtained in the reactions of $\text{B}_9\text{C}_2\text{H}_{11}^{2-}$ with lanthanide chlorides as compared to those of the d-transition metal chlorides. Also the types of products obtained in the reactions of NdCl_3 with $\text{B}_9\text{C}_2\text{H}_{11}^{2-}$ are different from those with Cp^- . Finally, differences are noted between the products of the reactions with NdCl_3 from those with ErCl_3 .

THE NdCl_3 -DICARBOLLIDE ION SYSTEMExperimentalMaterials

Anhydrous NdCl_3 (99.9%) was obtained from Rocky Mountain Research, Inc., Golden, Col., and was used as received.

$\text{Na}_2\text{B}_9\text{C}_2\text{H}_{11}$ was prepared by the reaction of NaH with $(\text{CH}_3)_3\text{NHB}_9\text{C}_2\text{H}_{12}$ [46]. The $(\text{CH}_3)_3\text{NHB}_9\text{C}_2\text{H}_{12}$ had been prepared by the selective base degradation of $\text{B}_{10}\text{C}_2\text{H}_{12}$ [45]. The carborane was either purchased from Alpha Inorganics, Inc., Beverly, Mass., or prepared from the permanganate oxidation of the carborane diester from the reaction of $\text{B}_{10}\text{H}_{14}$ with $\text{AcOCH}_2\text{CCCH}_2\text{OAc}$ in the presence of $(\text{CH}_3)_2\text{S}$ [66]. The crucial step in the synthesis is the oxidation. The rate of addition of the KMnO_4 should be 50 g/hr. The excess KMnO_4 must be destroyed immediately after the oxidation reaction as it will slowly destroy the product if allowed to stand.

NaH was purchased from Alpha Inorganics, Inc., Beverly, Mass., as a 50% dispersion in mineral oil.

All solvents were Reagent Grade or better and were distilled from LiAlH_4 under nitrogen immediately prior to use.

Preparation of $[\text{NaNdCl}_2(\text{B}_9\text{C}_2\text{H}_{11}) \cdot \text{THF}]_2 \cdot \text{NdCl}_3$, (I)

Five grams (20 mmoles) of anhydrous NdCl_3 were added to a solution of 10 mmoles $\text{Na}_2(\text{B}_9\text{C}_2\text{H}_{11})$ [45] containing excess NaH in 100 ml THF, contained in a 3-neck 250 ml round bottom flask equipped with a condenser and dry N_2 inlet. The mixture was gently refluxed with stirring overnight. Following filtration, the volume of the blue THF solution was reduced and pentane was slowly added until precipitation was complete. Excess THF was removed by pumping on the resulting light blue solid at 10^{-4} mm Hg at 25°C for two weeks. Calculated for $[\text{NaNdCl}_2(\text{B}_9\text{C}_2\text{H}_{11}) \cdot \text{THF}]_2 \cdot \text{NdCl}_3$: Nd, 38.01; Cl, 21.90; B, 17.13; C, 12.69; H, 3.37; Na, 4.05. Found: Nd, 38.99; Cl, 21.67; B, 17.53; C, 11.35; H, 3.98; Na, 4.14.

Complete elemental analysis on (I) was done by Schwartzkoff Microanalytical Laboratory, Woodside, N. Y.

A separate check on the THF content was done. The 12.7% found compared very well with the 12.66% calculated.

Because any name given (I) would be so unwieldy, it was not named.

Preparation of $\text{Na}_3\text{Nd}(\text{B}_9\text{C}_2\text{H}_{11})_3 \cdot 2\text{THF}$, (II)

The NdCl_3 and $(\text{CH}_3)_3\text{NHB}_9\text{C}_2\text{H}_{12}$ was carefully weighed to insure that the mole ratio of the reactants would be exactly 1:3.

Anhydrous NdCl_3 , 0.75 g (3.0 mmoles), was carefully added to a solution of 9.0 mmoles $\text{Na}_2\text{B}_9\text{C}_2\text{H}_{11}$ [45] containing excess NaH . Following the procedure described above, the excess THF was removed from the resulting deep powder blue solid by pumping at 10^{-4} mm Hg at 25°C for two weeks. Calculated for $\text{Na}_3\text{Nd}(\text{B}_9\text{C}_2\text{H}_{11})_3 \cdot 2\text{THF}$: Nd, 19.11; THF, 19.11; Na, 9.14. Found: Nd, 20.60; THF, 22.0; Na, 10.90. Absolutely no chloride was detected.

(II) is tentatively named sodium tris(dicarbollyl)neodimate(III) bis(tetrahydrofuran)adduct.

Reaction of $[\text{NaNdCl}_2(\text{B}_9\text{C}_2\text{H}_{11}) \cdot \text{THF}]_2\text{NdCl}_3$, (I), with $\text{Na}_2\text{B}_9\text{C}_2\text{H}_{11}$

In a Schlenk flask were placed 0.90 g (0.79 mmoles) (I) and 1.0 g (5.6 mmoles) $\text{Na}_2\text{B}_9\text{C}_2\text{H}_{11}$ and 50 ml of THF was vacuum transferred into the flask. The solution was stirred at room temperature for three hours. After filtration the THF was removed and the blue solid was shown to contain no chloride. No product was isolated but it was assumed to be $\text{Na}_3\text{Nd}(\text{B}_9\text{C}_2\text{H}_{11})_3 \cdot x\text{THF}$.

Attempted Reaction of $\text{Na}_3\text{Nd}(\text{B}_9\text{C}_2\text{H}_{11})_3 \cdot \text{THF}$, (III), with NdCl_3

Attempts to displace $\text{B}_9\text{C}_2\text{H}_{11}^{2-}$ from (III) with chloride using NdCl_3 proved fruitless. After stirring a solution of the reactants at

room temperature overnight, (III) was recovered unaltered.

Reaction of $[\text{NaNdCl}_2(\text{B}_9\text{C}_2\text{H}_{11}) \cdot \text{THF}]_2 \cdot \text{NdCl}_3$ (I), with NaCp

Several attempts were made to prepare a compound of the type $\text{NaNdCp}_2(\text{B}_9\text{C}_2\text{H}_{11}) \cdot x(\text{THF})$. In each case the Cp^- quantitatively displaced the chloride in (I) and one product was characterized as NaCp_3 . Infrared spectra of the other product(s) indicate the presence of both Cp^- and $\text{B}_9\text{C}_2\text{H}_{11}^{2-}$. However, no pure compound was isolated.

Analyses

Nd and THF were determined in the same manner as in Part I.

Chloride was determined by potentiometric titrations using a Corning Model #476126 Chloride Selective Electrode and a Chemtrix Type 60 pH meter operating on the mV scale. A 100 mg sample was hydrolyzed, acidified and diluted to 100 ml. The dicarbollide ions were destroyed by treating 10 ml aliquots with 20 ml of 30% H_2O_2 for two hours. The solutions were then titrated with standard $0.01\text{M } \text{Ag}^+$. The end point was taken as the point of maximum slope of the curve.

Na was determined by flame photometry techniques using a McKee-Paterson flame photometry station. The station was equipped with a MP-1023-A aspirator burner, MP-1018 monochrometer, MP-1021 photomultiplier tube and MP-1002 power supply Solutions containing between 1-3 ppm were used.

Aqueous solutions consistently gave low results. Apparently there is some decomposition during hydrolysis as a film was formed on the walls of the hydrolysis vessel. This film may in some manner preferentially adsorb Na ions. A qualitative flame test of this film gave a positive Na test.

When samples were dissolved in ethanol, satisfactory results were obtained and no film was observed.

Physical Measurements

Infrared spectra and X-ray powder patterns were obtained in the same manner as in Part I.

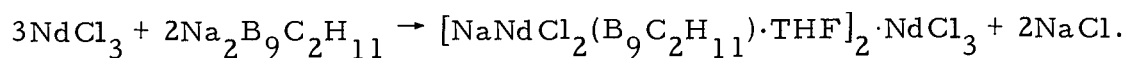
Visible spectra of THF solutions were recorded on a Cary 14 spectrophotometer using 1 cm silica cells.

The ^{11}B nmr were recorded on a Varian HA-100 at 32.1 MHz using $\text{BF}_3 \cdot \text{O}(\text{C}_2\text{H}_5)_2$ as an external standard.

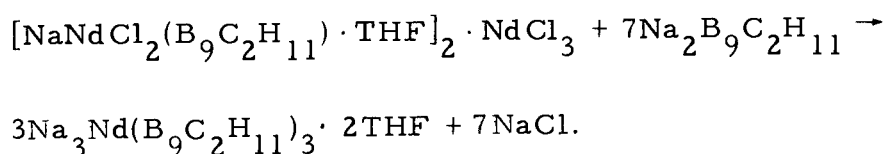
Summary

When mole ratios of NdCl_3 to $\text{Na}_2\text{B}_9\text{C}_2\text{H}_{11}$ of 2:1 or greater were used the product isolated was $[\text{NaNdCl}_2(\text{B}_9\text{C}_2\text{H}_{11}) \cdot \text{THF}]_2 \cdot \text{NdCl}_3$, (I).

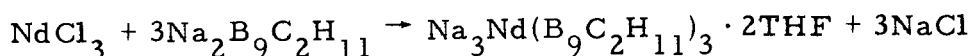
The equation for the reaction is



Because of the "extra" NdCl_3 in (I) we were concerned that the product was a mixture. An X-ray powder diffraction pattern shows no lines due to NdCl_3 , thus clearly indicating that (I) is not a mixture containing NdCl_3 , Table 10. $\text{Na}_2\text{B}_9\text{C}_2\text{H}_{11}$ further reacts with (I) to displace all the chloride and give $\text{Na}_3\text{Nd}(\text{B}_9\text{C}_2\text{H}_{11})_3 \cdot 2\text{THF}$, (II) according to the equation



(II) can more readily be prepared according to the equation



These reactions clearly demonstrate that the products are dependent on the mole ratios of the reactants and that the displacement of chloride from NdCl_3 by $\text{B}_9\text{C}_2\text{H}_{11}^{2-}$ is a stepwise process. This displacement reaction is irreversible, however. Attempts to displace the $\text{B}_9\text{C}_2\text{H}_{11}^{2-}$ from (II) using NdCl_3 proved fruitless. In fact, (II) was recovered unaltered.

The reaction of (I) with NaCp was rapid and was expected to proceed according to the equation

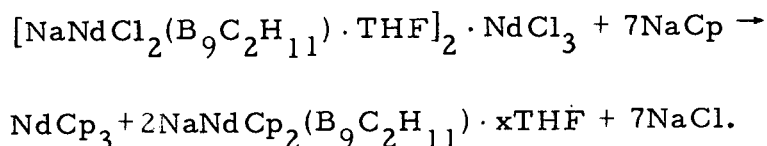


Table 10. Powder pattern data^a for dicarbollide compounds.

NdCl_3^b	$[\text{NaNdCl}_2(\text{B}_9\text{C}_2\text{H}_{11}) \cdot \text{THF}]_2 \cdot \text{NdCl}_3$	$\text{Na}_2(\text{B}_9\text{C}_2\text{H}_{11})$	$\text{NaErCl}_2(\text{B}_9\text{C}_2\text{H}_{11}) \cdot \text{THF}$	ErCl_3^c
	11.99 (s)		11.71 (s)	
			8.55 (w)	
	7.83 (w)		7.65 (w)	
	7.14 (m)		7.03 (m)	
6.42	6.22 (m)		6.09 (m)	6.09
	5.92 (w)	6.06 -	5.76 (w)	
		5.39 (s)		
		5.48 (vs)		
	5.19 (m)	5.16 (w)		
		4.55 (w)		
		3.84 (w)	3.89 (w)	
3.54				3.38
2.56				2.74
2.11				
	2.01 (s)	1.99 (m)	2.00 (m)	
				1.88

^as = strong, m = medium, w = weak, d-spacing calculated using the Bragg equation.

^bSee reference [67].

^cSee reference [68].

The solution was filtered and the white solid was analyzed for chloride. This analysis showed that the displacement of chloride from (I) was complete. NdCp_3 was isolated by sublimation and identified by its infrared and visible spectra [31,32]. Although no pure product of the type $\text{NaNdCp}_2(\text{B}_9\text{C}_2\text{H}_{11})$ was isolated the infrared spectrum of the product which remained after sublimation indicated the presence of both Cp^- and $\text{B}_9\text{C}_2\text{H}_{11}^{2-}$.

The infrared spectra of (I) and (II) are virtually identical. Each spectrum contains an intense broad band centered at about 2520 cm^{-1} and bands at 2965, 2890, 1005 and 862 cm^{-1} . No other strong bands are observed. The 2520 cm^{-1} band is in the characteristic B-H stretching region and most certainly is due to the B-H stretching in the dicarbollide ion. Strong bands in this region are also seen for d-transition metal dicarbollides [46]. The other bands are due to the C-H stretching, C-O stretching and C-H bending modes of the THF's.

The visible spectra of (I) and (II) are virtually identical with the spectrum of NdCl_3 , Table 11. The spectra demonstrate the characteristic Nd^{3+} bands and differ only slightly from the spectra of aqueous Nd^{3+} [69].

The ^{11}B nmr of (I) has the same pattern as $(\text{CH}_3)_3\text{NHB}_9\text{C}_2\text{H}_{12}$ with very nearly the same chemical shifts and coupling constants, Table 12.

Table 11. Visible spectra^a of dicarbollide compounds.

NdCl ₃	(I)	(II)	(III)	(IV)	ErCl ₃
743 (m, br)	745 (m, br)	750 (m, br)	655 (w)	655 (w)	652 (vw)
594 (sh)	593 (sh)	592 (s)	542 (vw)		530 (w, sh)
585 (s)	586 (s)	584 (sh)	522 (s)	522 (s)	518 (s)
577 (m)	580 (sh)		488 (w)	490 (w)	488 (w)
			452 (w)		
529 (w)	528 (w)	535 (w, br)	408 (w)		
515 (w)	515 (w)				

(I) = [NaN₂Cl₂(B₉C₂H₁₁) · THF]₂ · NdCl₃.

(II) = Na₃Nd(B₉C₂H₁₁)₃ · 2THF.

(III) = NaErCl₂(B₉C₂H₁₁) · THF.

(IV) = Na₃Er(B₉C₂H₁₁)₃ · THF.

^as = strong, m = medium, w = weak, vw = very weak, sh = shoulder, br = broad.

Table 12. ^{11}B nmr data.

Compound	Shift	J	Area
$(\text{CH}_3)_3\text{NH}(\text{B}_9\text{C}_2\text{H}_{12})^{\text{a}}$	+10.9	141	2.0
	+16.3	140	3.0
	+21.0	138	2.1
	+32.1	128	1.0
	+36.5	131	1.0
$(\text{CH}_3)_3\text{NH}(\text{B}_9\text{C}_2\text{H}_{12})^{\text{b}}$	+16.6	147	2.0
	+22.9	147	3.0
	+27.8	133	2.0
	+38.7	133	1.0
	+43.4	133	1.0
$[\text{NaNdCl}(\text{B}_9\text{C}_2\text{H}_{11}) \cdot \text{THF}]_2 \cdot \text{NdCl}_3$	+15.0	145	2.0
	+20.6	173	3.0
	+25.6	145	2.0
	+37.1	106	1.0
	+40.8	132	1.0
$\text{NaErCl}_2(\text{B}_9\text{C}_2\text{H}_{11}) \cdot \text{THF}$	+20.5	174	2.0
	+26.2	174	3.0
	+31.8	157	2.0
	+43.6	116	1.0
	+48.0	145	1.0

^aSee reference [45].^bThis work.

THE ErCl_3 -DICARBOLLIDE ION SYSTEMExperimentalMaterials

Anhydrous ErCl_3 (99.9%) was obtained from Rocky Mountain Research, Inc., Golden, Col., and was used as received.

All other materials were the same as in the NdCl_3 -dicarbollide ion system.

Preparation of $\text{NaErCl}_2(\text{B}_9\text{C}_2\text{H}_{11}) \cdot \text{THF}$, (III)

Anhydrous ErCl_3 , 7.47 g (20 mmoles), was added to a solution of 10 mmoles $\text{Na}_2(\text{B}_9\text{C}_2\text{H}_{11})$ [45] containing excess NaH. Following the procedure described above, the resulting light pink solid was washed several times with cyclohexane and dried at 10^{-4} mm Hg at 25°C for two weeks. Calculated for $\text{NaErCl}_2(\text{B}_9\text{C}_2\text{H}_{11}) \cdot \text{THF}$: Er, 35.92; Cl, 15.23; Na, 4.94; THF, 15.48. Found: Er, 35.46; Cl, 14.62; Na, 4.62; THF, 17.4. Complete elemental analyses of (III), done by Schwartzkoff Microanalytical Laboratory gave unsatisfactory results. Only 86% of the total composition was found. B and Na, calculated 20.89 and 4.94 and found 13.30 and 3.37, respectively, gave the most unsatisfactory results. Warren and Hawthorne often were unable to obtain satisfactory analyses on several d-transition

metal dicarbollides [51]. B in particular was often unsatisfactory.

We suspect then in our case the low B results may be due in part to the formation of erbium borides which are known to be refractory and unreactive.

(III) is tentatively named sodium diclorodicarbollylerbate(III) tetrahydrofuran adduct.

Preparation of $\text{Na}_3\text{Er}(\text{B}_9\text{C}_2\text{H}_{11})_3 \cdot \text{THF}$, (IV)

The ErCl_3 and $(\text{CH}_3)_3\text{NHB}_9\text{C}_2\text{H}_{12}$ were carefully weighed to insure that the mole ratio of the reactants would be exactly 1:3. Anhydrous ErCl_3 , 0.82 g (3.0 mmoles), was carefully added to a solution of 9.0 mmoles $\text{Na}_2\text{B}_9\text{C}_2\text{H}_{11}$ [45] containing excess NaH. Following the procedure described above, the excess THF was removed from the resulting deep pink solid by pumping at 10^{-4} mm Hg at 25°C for two weeks. Calculated for $\text{Na}_3\text{Er}(\text{B}_9\text{C}_2\text{H}_{11})_3 \cdot \text{THF}$: Er, 22.71; THF, 10.22; Na, 9.78. Found: Er, 22.70; THF, 10.5; Na, 10.80. Absolutely no chloride was detected.

(IV) is tentatively named sodium tris(dicarbollyl)erbate(III) tetrahydrofuran adduct.

Attempted Reaction of $\text{Na}_3\text{Er}(\text{B}_9\text{C}_2\text{H}_{11})_3 \cdot \text{THF}$, (IV), with ErCl_3

Attempts to displace $\text{B}_9\text{C}_2\text{H}_{11}^{2-}$ from (IV) using ErCl_3 proved fruitless. After stirring mixtures of the reactants at room temperature overnight, (IV) was recovered unaltered.

Reaction of $\text{NaErCl}_2(\text{B}_9\text{C}_2\text{H}_{11}) \cdot \text{THF}$, (II), with NaCp

As in the reaction of (I) with NaCp , Cp^- quantitatively displaces the chloride in (II). Nothing sublimed at 225°C at 10^{-4} mm Hg indicating that no ErCp_3 was formed. The infrared spectrum of the product indicated the presence of both Cp^- and $\text{B}_9\text{C}_2\text{H}_{11}^{2-}$. However no pure product was isolated.

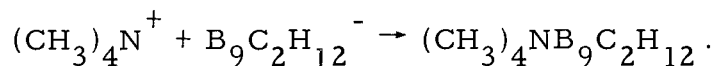
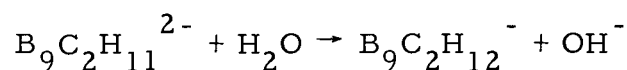
Thermal Decomposition of $\text{NaErCl}_2(\text{B}_9\text{C}_2\text{H}_{11}) \cdot \text{THF}$, (II)

After a sample of (II) was heated to 70°C at 10^{-4} mm Hg, the solid was no longer totally soluble in THF and had a Cl^- to Er^{3+} ratio of 1.8. Heating (II) to 140°C caused the pink solid to turn yellow. This yellow solid was totally insoluble in THF.

Analyses

Er, Cl, Na and THF were determined in the manner previously described.

In addition an attempt was made to analyze the $\text{B}_9\text{C}_2\text{H}_{11}^{2-}$ by precipitating it from aqueous solution as $(\text{CH}_3)_4\text{NB}_9\text{C}_2\text{H}_{12}$ according to the equations



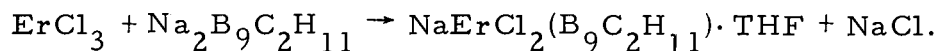
A sample was hydrolyzed, acidified and added to a solution of $(\text{CH}_3)_4\text{NCl}$. Seventy percent of the dicarbollide was recovered by this procedure. The film which formed on the hydrolysis vessel walls also gave a positive flame test for boron as well as Na.

Physical Measurements

The infrared, visible and ^{11}B nmr spectra and X-ray powder patterns were obtained in the manner previously described.

Summary

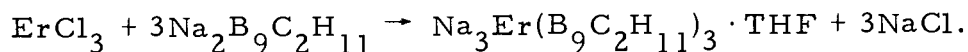
$\text{NaErCl}_2(\text{B}_9\text{C}_2\text{H}_{11}) \cdot \text{THF}$, (III) was isolated as the reaction product when mole ratios of ErCl_3 to $\text{Na}_2\text{B}_9\text{C}_2\text{H}_{11}$ were 2:1 or greater. The equation for the reaction is



An X-ray powder pattern of the product shows no ErCl_3 to be present.

$\text{Na}_3\text{Er}(\text{B}_9\text{C}_2\text{H}_{11})_3 \cdot \text{THF}$ (IV) was isolated when the mole ratio is 1:3.

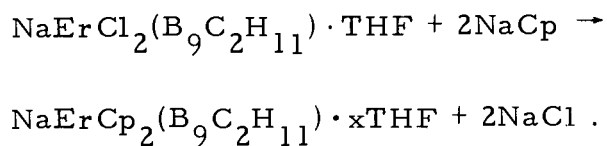
The equation for the reaction is



These reactions demonstrate that the products are dependent on the mole ratios of the reactants.

As in the NdCl_3 system, the displacement of chloride by dicarbollide is irreversible. Attempts to displace the $\text{B}_9\text{C}_2\text{H}_{11}^{2-}$ from (IV) using ErCl_3 proved fruitless and (IV) was recovered unaltered.

NaCp was expected to react with (II) according to the equation



After treating (II) with NaCp and filtering, no chloride was present in the soluble product. No pure product was isolated but the infrared spectrum indicated the presence of both Cp^- and $\text{B}_9\text{C}_2\text{H}_{11}^{2-}$. In addition ErCp_3 was shown to be absent because nothing sublimed.

The infrared spectra of (III) and (IV) are identical with the compounds isolated in the NdCl_3 system. The only information they offer is to confirm the presence of a B-H stretch ($2500\text{-}2550\text{ cm}^{-1}$)

and the THF (2965, 1010 and 860 cm^{-1}).

The visible spectra of (III) and (IV) are virtually identical with that of ErCl_3 , Table 11. The spectra show the characteristic Er^{3+} bands and differ only slightly from the spectra of aqueous Er^{3+} [69].

The ^{11}B nmr of (II) has the same pattern as $(\text{CH}_3)_3\text{NHB}_9\text{C}_2\text{H}_{12}$ with very nearly the same chemical shifts and coupling constants, Table 12.

DISCUSSION AND CONCLUSIONS

The first reaction done in this study was that of NdCl_3 with $\text{B}_9\text{C}_2\text{H}_{11}^{2-}$ in mole ratios of 2:1 or greater. The NdCl_3 was added in excess because it could easily be removed by filtration. The product of the reaction was expected to be of the type $\text{Na}_3\text{Nd}(\text{B}_9\text{C}_2\text{H}_{11})_3 \cdot x\text{THF}$. The reasons for this expectation were twofold. First, the dicarbollide has been shown to behave similarly to Cp^- in its reactions with d-transition metal chlorides by Hawthorne and coworkers [50]. Second, the reaction of NdCl_3 with Cp^- was known to give only NdCp_3 [31]. To our surprise however, the product isolated was $[\text{NaNdCl}_2(\text{B}_9\text{C}_2\text{H}_{11}) \cdot \text{THF}]_2 \cdot \text{NdCl}_3$, (I).

The presence of chloride in (I) indicates that the reaction of NdCl_3 with $\text{B}_9\text{C}_2\text{H}_{11}^{2-}$ differs dramatically from that of the d-transition metal chlorides with $\text{B}_9\text{C}_2\text{H}_{11}^{2-}$ in which all the chloride is displaced. This difference can be accounted for by comparing the bonding in the d-transition metal dicarbollide compounds to that in (I). Consider for the moment $[\text{Fe}(\text{B}_9\text{C}_2\text{H}_{11})_2]^-$, for example. The ^{11}B nmr of this compound shows boron resonances from -101 to +462 ppm with respect to $\text{BF}_3 \cdot \text{O}(\text{C}_2\text{H}_5)_2$ [46]. These large shifts are explained in terms of high overlap between the d-orbitals of the paramagnetic Fe^{3+} and the π -orbitals of the dicarbollide. In other words the bonding between the Fe^{3+} and the dicarbollide ligands is largely covalent.

This covalent bond is energetically more favorable than an ionic Fe-Cl bond and thus all the Cl^- is readily displaced by $\text{B}_9\text{C}_2\text{H}_{11}^{2-}$. In sharp contrast to this, the ^{11}B nmr for (I) shows resonances from only 15 to 40 ppm and are essentially identical to those observed for ionic $(\text{CH}_3)_3\text{NHB}_9\text{C}_2\text{H}_{12}$, Table 12. Therefore, the ^{11}B nmr indicates that only an ionic interaction exists between $\text{B}_9\text{C}_2\text{H}_{11}^{2-}$ and Nd^{3+} . Also, the visible spectrum of (I) shows no perturbation on the Nd^{3+} ion, Table 11.

Sharp differences are also noted between the reactions of NdCl_3 with $\text{B}_9\text{C}_2\text{H}_{11}^{2-}$ and with Cp^- . With Cp^- , only NdCp_3 is formed regardless of the mole ratios of the reactants [22,23]. With $\text{B}_9\text{C}_2\text{H}_{11}^{2-}$, the products are dependent on the mole ratios of the reactants and a significant number of undisplaced chlorides are present in (I). Only when (I) is treated with more $\text{B}_9\text{C}_2\text{H}_{11}^{2-}$ or when NdCl_3 and $\text{B}_9\text{C}_2\text{H}_{11}^{2-}$ are reacted in a 1:3 mole ratio is a chloride free product, $\text{Na}_3\text{Nd}(\text{B}_9\text{C}_2\text{H}_{11})_3 \cdot 2\text{THF}$, (II), obtained. This result is unexpected because if one thinks of these reactions as strictly ionic, then $\text{B}_9\text{C}_2\text{H}_{11}^{2-}$ should displace chloride more readily than Cp^- , because of its higher charge.

ErCl_3 reacts with $\text{B}_9\text{C}_2\text{H}_{11}^{2-}$ to give $\text{NaErCl}_2(\text{B}_9\text{C}_2\text{H}_{11}) \cdot \text{THF}$, (III), or $\text{Na}_3\text{Er}(\text{B}_9\text{C}_2\text{H}_{11})_3 \cdot \text{THF}$, (IV) when the mole ratios of the reactants are 2:1 or 1:3, respectively. One can see that the products of the ErCl_3 reactions are not the same as those of NdCl_3 under the

same reaction conditions. In particular, the "extra" NdCl_3 in (I) has no analog in (III) and the chloride free product in the NdCl_3 system, (II), contains two THF molecules while that in the ErCl_3 system, (IV), contains only one. We suggest that these differences are caused by the lanthanide contraction.

As mentioned in the introduction, one of the consequences of the lanthanide contraction is a change in the coordination spheres of the metal in going from compounds of light to heavy lanthanides due to their smaller ionic sizes. Thus we suspect that the Nd compounds in the present work are more highly coordinated than those of Er. This seems apparent when comparing $\text{Na}_3\text{Nd}(\text{B}_9\text{C}_2\text{H}_{11})_3 \cdot 2\text{THF}$ with $\text{Na}_3\text{Er}(\text{B}_9\text{C}_2\text{H}_{11})_3 \cdot \text{THF}$, where the additional solvent molecule present in the former is most likely coordinated to the Nd^{3+} . Alternatively, if the Nd^{3+} coordination sphere is completely occupied by the dicarbollide ions, the THF could occupy a space in the solid created because of the larger size of the Nd^{3+} .

The comparison of $[\text{NaNdCl}_2(\text{B}_9\text{C}_2\text{H}_{11}) \cdot \text{THF}]_2 \cdot \text{NdCl}_3$, (I), with $\text{NaErCl}_2(\text{B}_9\text{C}_2\text{H}_{11}) \cdot \text{THF}$, (II), is not so simple. If the Nd product merely contained an additional THF as compared to the Er product, as is the case with (II) and (IV), then the Nd product in this case would have been $\text{NaNdCl}_2(\text{B}_9\text{C}_2\text{H}_{11}) \cdot 2\text{THF}$, (V). We suggest that the "extra" NdCl_3 in (I) is present as part of a complex chloride bridged system. The geometry of this system would be such that a more

satisfactory coordination sphere would exist around each Nd^{3+} than if the product were (V). The larger size of Nd^{3+} may well be the reason for the difference observed between (I) and (III).

X-ray structure determinations of these compounds would be most enlightening. Unfortunately, we were unable to grow crystals of any of the compounds discussed in Part II.

BIBLIOGRAPHY

1. P.S. Skell and L.D. Wescott, J. Am. Chem. Soc., 85, 1023 (1963).
2. P.L. Timms, Adv. in Inorg. Chem. and Radiochemistry, 14, 121 (1972).
3. P.S. Skell, J.J. Havel and M.J. McGlinchey, Accts. Chem. Res., 6, 97 (1973).
4. G.A. Ozin and A. VanderVolt, Accts. Chem. Res., 6, 313 (1973).
5. Thirteen papers presented at the symposium are presented in Angew. Chem. Internat. Edit. Eng., 14, 193-221, 273-321 (1975).
6. R.E. Honig in "The Characterization of High Temperature Vapors" (J.L. Margrave, ed), p. 475. Wiley, New York, 1967.
7. P.S. Skell and R.R. Engel, J. Am. Chem. Soc., 88, 3749 (1966).
8. P.S. Skell, D.L. Williams-Smith and M.J. McGlinchey, J. Am. Chem. Soc., 95, 3337 (1973).
9. F.W.S. Benfield, M.L.H. Green, J.S. Ogden and D. Young, J. C.S. Chem. Comm., 866 (1973).
10. E.M. Van Dam, W.N. Brent, M.P. Silvon and P.S. Skell, J. Am. Chem. Soc., 97, 465 (1975).
11. U. Muller-Westerhoff and A.D. Streitwieser, J. Am. Chem. Soc., 90, 7364 (1968).
12. For literature prior to 1971, see R.G. Hayes and J.L. Thomas, Organometal. Chem. Rev. A, 7, 1 (1971). Annual surveys have been published. For 1971, see F. Calderazzo, J. Organometal. Chem. 53, 173 (1973). For 1972, see F. Calderazzo, *ibid.*, 79, 175 (1974). For 1973, see T.J. Marks, *ibid.*, 79, 181 (1974).
13. K.O. Hodgson, F. Mares, P.F. Starks and A. Streitwieser, J. Am. Chem. Soc., 95, 8650 (1973).

14. A. Streitwieser, U. Muller-Westerhoff, G. Sonnichsen, F. Mares, D.G. Morrell, K.O. Hodgson and C.A. Harmon, J. Am. Chem. Soc., 95, 8644 (1973).
15. M. Tsutsui and N. Ely, J. Am. Chem. Soc., 96, 3650 (1974).
16. M. Tsutsui and N. Ely, J. Am. Chem. Soc., 96, 4042 (1974).
17. A.E. Gebala and M. Tsutsui, J. Am. Chem. Soc., 95, 91 (1973).
18. T.J. Marks, A.M. Seyam and J.R. Kolb, J. Am. Chem. Soc., 95, 5529 (1973).
19. J.L. Slater, T.C. DeVore and V. Calder, Inorg. Chem., 12, 1918 (1973); 13, 1808 (1974).
20. Dean A. Van Leirsburg, PhD Dissertation, Oregon State University, Corvallis, 1974.
21. Chemical and Engineering News, Dec. 26, 1973, p. 26.
22. S. Masnatskyj, R.E. Maginn and M. Dubeck, Inorg. Chem., 2, 904 (1963).
23. R.E. Maginn, S. Masnatskyj and M. Dubeck, J. Am. Chem. Soc., 85, 672 (1963).
24. R.G. Hayes and J.L. Thomas, J. Am. Chem. Soc., 91, 6876 (1969).
25. K.O. Hodgson and K.N. Raymond, Inorg. Chem., 11, 3030 (1972).
26. K.O. Hodgson and K.N. Raymond, Inorg. Chem., 11, 171 (1972).
27. J.D. Jamerson, A.P. Masino and J. Takats, J. Organometal. Chem., 65, C33 (1974).
28. H. Breil and G. Wilke, Angew. Chem. internat. Edit. Eng., 5, 898 (1966).
29. H. Dietrich and H. Dreiks, Angew. Chem. internat. Edit. Eng., 5, 899 (1966).

30. A. Avdeef, K.N. Raymond, K.O. Hodgson and A. Zalkin, *Inorg. Chem.*, 11, 1083 (1972).
31. J.M. Birmingham and G. Wilkinson, *J. Am. Chem. Soc.*, 78, 42 (1956).
32. For infrared spectra of lanthanide cyclopentadienide complexes, see for example, E.O. Fischer and H. Fischer, *J. Organometal. Chem.*, 3, 181 (1965) and F. Calderazzo, R. Pappalardo and S. Losi, *J. Inorg. Nucl. Chem.*, 28, 987 (1966).
33. G. Schwarzenbach, "Complexometric Titrations," 1st ed., Methuen, Great Britain, 1957.
34. Programs used for the Data General Corporation NOVA computer were those of the Syntex Analytical Instruments software package.
35. D.T. Cromer and J.B. Mann, *Acta Crystallogr., Sec. A*, 24, 321 (1968).
36. "International Tables for X-ray Crystallography," The Kynoch Press, Birmingham, England, 1962.
37. R.D. Shannon and C.T. Prewitt, *Acta Crystallogr. Sect. B*, 25, 925 (1969); 26, 1046 (1970).
38. J.L. Atwood, C.F. Haines, Jr., M. Tsutsui and A.E. Gebala, *J.C.S. Chem. Comm.*, 452 (1973); *Proc. Sixth Int. Conf. Organometal. Chem.*, Amherst, Mass., 155 (1973).
39. E.R. Lippincott and D.R. Nelson, *J. Chem. Phys.*, 21, 1307 (1953).
40. W.T. Carnall and P.R. Fields, *Advan. Chem. Sec.*, No. 71 (1967).
41. H.P. Fritz and H. Keller, *Chem. Ber.*, 95, 158 (1962).
42. T.L. Heying, J.W. Ager, Jr., S.L. Clark, D.J. Mangold, H.L. Goldstein, M. Hillman, R.J. Polak and J.W. Szymanski, *Inorg. Chem.*, 2, 1089 (1963).
43. J.A. Potenza and W.N. Libscomb, *Inorg. Chem.*, 3, 1673 (1964).

44. R.M. Adams, *Inorg. Chem* , 7, 1945 (1968).
45. M.F. Hawthorne, D.C. Young, P.M. Garrett, D.A. Owen, S.G. Schwerin, F.N. Tebbe and P.A. Wegner, *J. Am. Chem. Soc.* , 90, 862 (1968).
46. M.F. Hawthorne, D.C. Young, T.D. Andrews, D.V. Howe, R.L. Pilling, A.D. Pitts, M. Reintjes, L.F. Warren and P.A. Wegner, *J. Am. Chem. Soc.* , 90, 879 (1968).
47. E.B. Moore, L.L. Lohr and W.N. Lipscomb, *J. Chem. Phys.* , 35, 1329 (1961).
48. M.F. Hawthorne, D.C. Young and P.A. Wegner, *J. Am. Chem. Soc.* , 87, 1818 (1965).
49. A. Zalkin, T.E. Hopkins and D.H. Templeton, *Inorg. Chem.* , 6, 1911 (1967).
50. R.N. Grimes, "Carboranes", Academic Press, New York, N.Y., 1970.
51. Leslie F. Warren, PhD Dissertation, University of California, Riverside, 1969.
52. M.F. Hawthorne and G.B. Dunks, *Science* , 178, 462 (1972).
53. M.F. Hawthorne, K.P. Callahan and R.J. Wiersema, *Tetrahedron* , 30, 1795 (1974).
54. K.P. Callahan, W.J. Evans and M.F. Hawthorne, *Ann. N.Y. Acad. Sci.* , 239, 88 (1974).
55. D.A. Owen and M.F. Hawthorne, *J. Am. Chem. Soc.* , 93, 873 (1971).
56. L.F. Warren, Jr. and M.F. Hawthorne, *J. Am. Chem. Soc.* , 92, 1157 (1970).
57. C.S. Salentine and M.F. Hawthorne, *J. Am. Chem. Soc.* , 97, 426 (1975).
58. F.Y. Lo, C.E. Strouse, K.P. Callahan, C.B. Knobler and M.F. Hawthorne, *J. Am. Chem. Soc.* , 97, 428 (1975).

59. T.E. Paxson and M.F. Hawthorne, J. Am. Chem. Soc., 96, 4674 (1974).
60. E.L. Hoel and M.F. Hawthorne, J. Am. Chem. Soc., 96, 4676 (1974).
61. E.L. Hoel and M.F. Hawthorne, J. Am. Chem. Soc., 95, 2712 (1973).
62. E.L. Hoel and M.F. Hawthorne, J. Am. Chem. Soc., 96, 6770 (1974).
63. A.R. Siedle, J. Organometal Chem., 90, 249 (1975).
64. W.H. Zachariasen, J. Chem. Phys., 16, 254 (1948).
65. D.H. Templeton and G.F. Carter, J. Phys. Chem., 58, 940 (1954).
66. C.R. Kutal, D.A. Owen and L.J. Todd, Inorganic Syntheses, 11, 19 (1968).
67. Nat. Bur. Standards (U.S.) Mono. 25, Sec. 1, 1961.
68. F. Weigel and V. Wishnevsky, Chem. Ber., 103, 193 (1970).
69. W. Prandtl and K. Scheiner, Z. anorg. u. allegem. Chem., 220, 107 (1934).

APPENDIX

PLEASE NOTE:

The following pages contain
very tiny print. Filmed as
received.

UNIVERSITY MICROFILMS

Table with 10 columns: L, FOM SO DEL, L, FOM SO DEL, L, FOM SO DEL, L, FOM SO DEL, L, FOM SO DEL. The table contains numerical data for various categories, likely related to astronomical observations or measurements. The data is organized in a grid-like structure with multiple rows and columns.

OBSERVED STRUCTURE FACTORS FOR NO2 COT3 THF2 DEKOCK, ELY AND HOPKINS
(CONTINUED)
PAGE 2

[illegible]